Identification of *FoxP* circuits involved in locomotion and object fixation in *Drosophila*

Ottavia Palazzo, Mathias Raß, Björn Brembs*

Universität Regensburg, Institut für Zoologie - Neurogenetik, Regensburg, Germany

*bjoern@brembs.net

Abstract

The *FoxP* family of transcription factors is necessary for operant self-learning, an evolutionary conserved form of motor learning. The expression pattern, molecular function and mechanisms of action of the *Drosophila FoxP* orthologue remain to be elucidated. By editing the genomic locus of *FoxP* with CRISPR/Cas9, we find that the three different *FoxP* isoforms are expressed in neurons, but not in glia and that not all neurons express all isoforms. Furthermore, we detect *FoxP* expression in, e.g., the protocerebral bridge, the fan shaped body and in motorneurons, but not in the mushroom bodies. Finally, we discover that *FoxP* expression during development, but not adulthood, is required for normal locomotion and landmark fixation in walking flies. While *FoxP* expression in the protocerebral bridge and motorneurons is involved in locomotion and landmark fixation, the *FoxP* gene can be deleted from dorsal cluster neurons and mushroom-body Kenyon cells without affecting these behaviors.

1. Introduction

The family of *Forkhead Box* (*Fox*) genes comprises a large number of transcription factors that share the evolutionary conserved forkhead/winged-helix DNA-binding domain (Hannenhalli and Kaestner, 2009). In mammals, the *FoxP* subfamily (*FoxP1-4*) members (Santos et al., 2011) are abundantly expressed during the development of multiple cell types, such as cardiomyocytes, neurons, lung epithelial secretory cells and T-cells (Golson and Kaestner, 2016). In particular, *FoxP1* and *FoxP2* have generated interest because of their roles in regulating the development of cognitive processes such as speech and language acquisition (Bolhuis, 2011; Carr et al., 2010; Co et al., 2020; den Hoed and Fisher, 2020; Hagoort, 2019; Horn et al., 2010; Lai et al., 2001; Morgan et al., 2016; Reuter et al., 2017; Schatton and Scharff, 2016).

Humans with *FOXP1* deletions present with mild mental retardation, delayed onset of walking, gross motor impairments and significant language and speech deficits (Horn et al., 2010). Mutations in *FOXP2* cause a severe speech and language disorder characterized by deficits in language processing, verbal dyspraxia and impaired grammatical skills,

without affecting other traits severely (den Hoed and Fisher, 2020; Lai et al., 2001). The function of *FoxP* genes in vocal learning appears to be evolutionary conserved as knockouts of the zebra finch orthologue of human *FOXP2* during the critical song learning period alters the structure of the crystallized song in the adults (Haesler et al., 2007). Such vocal learning is a form of motor learning that proceeds slowly from highly variable 'babbling' (in humans) and 'subsong' (in zebra finches) towards more stereotypic language and crystallized song, respectively. This specific kind of learning has been classified as a form of operant learning (Fee, 2014; Marler, 1991; Naour, 2009). It was recently shown that, as in humans and zebra finches, also in flies, *FoxP* is involved in such operant learning (Mendoza et al., 2014).

The original *forkhead* (*fkh*) gene was identified in the fruit fly *Drosophila melanogaster (Weigel et al., 1989)*, where mutations cause defects in head fold involution during embryogenesis, causing the characteristic "fork head". In contrast to chordates with four *FoxP* family members, only one orthologue of the *FoxP* subfamily is present in flies (*dFoxP*). The *dFoxP* gene gives rise to three different transcripts by alternative splicing (Castells-Nobau et al., 2019; Mendoza et al., 2014; Santos et al., 2011): *FoxP-*

isoform A (*FoxP-iA*), FoxP-isoform B (*FoxP-iB*) and FoxP-isoform IR (Intron Retention; *FoxP-iIR*) (Fig. 1A). The currently available reports as to the expression pattern of the *FoxP* gene have been contradictory and nothing is known as to whether the different isoforms are differentially expressed in different cell types. To resolve these issues we have tagged the endogenous *FoxP* gene, analyzed the isoform-specific expression patterns and compared them with the expression of a selection of cell-type specific markers.

Flies with a mutated *FoxP* gene not only show impairments in operant learning but also in motor coordination and performance of inborn behaviors (Castells-Nobau et al., 2019; Kottler et al., 2019; Lawton et al., 2014; Mendoza et al., 2014). While isoform-specific alleles did show different phenotypes as well as different degrees of severity of these impairments, it remains unknown which neurons require *FoxP* expression at what developmental stage(s) for normal locomotor behavior. We therefore knocked out the *FoxP* gene in a spatiotemporally controlled manner and analyzed spatial and temporal parameters of locomotor behavior in the resulting mutants in Buridan's paradigm.

2. Materials and Methods

2.1. Fly strains

Fly stocks were maintained at 18 °C (Table 1). Before experimental use, flies were kept at 25 °C, in a 12/12 hours light/dark regime at 60% relative humidity for at least one generation. All crosses were raised at 25 °C (except for the ones involving the temperature sensitive Gal4 inhibitor Gal80^{ts} *(McGuire et al., 2004, 2003)* that were raised at 18 °C) using 4-6 females and 2-4 males. For expression pattern visualizations, the *FoxP-iB-Gal4* and *FoxP-LexA* driver line, respectively, were crossed with the apropriate effector lines containing different GFP or RFP variants (Table 1). For behavioral analysis involving the *UAS-t:gRNA(4xFoxP)* effector line we crossed it first with *UAS-Cas9*, and subsequently with the appropriate driver line for each experiment (*ELAV-Gal4*, *D42-Gal4*, *C380-Gal4, cmpy-Gal4, ato-Gal4* and *ELAV-Gal4;Tub-Gal80^{ts}*).

For conditional knock-out experiments, two genetic constructs need to be brought together for the method to work effectively. The endonuclease Cas9 needs to be present as well as the guide RNA (gRNA) to provide a target for the nuclease. Hence, the appropriate control groups express only one component of the CRISPR/Cas9 combination. One line drives expression only of the Cas9 endonuclease (i.e.,

xxx-Gal4>UAS-Cas9, without gRNAs) and the other drives expression only of the gRNAs (i.e., *xxx-Gal4>UAS-t:gRNA(4xFoxP)* without Cas9). In this fashion, each strain not only controls for potential insertion effects of the transgenes used, but also for potential detrimental effects of expressing the components alone, irrespective of the excision of the target gene.

For the behavioral analysis involving the *FoxP-KO* mutant and the *FoxP-iB-Gal4* driver line we crossed the lines back into *Wild Type Berlin* genetic background for at least six generations in order to get the same genetic background as the *WTB* control.

Genotype	Use
;;;ok107-Gal4	driver line
;;ato-Gal4	driver line
;;C380-Gal4	driver line
;;cmpy-Gal4	driver line
;;D42-Gal4;	driver line
*;;FoxP-/-; **	mutant
*;;FoxP-iB-Gal4; **	driver line
*;;FoxP-LexA; **	driver line
;;Tdc2-Gal4;	driver line
*;;UAS-t:gRNA(4xFoxP); **	effector line
;ELAV-Gal4;;	driver line
;LexAop-mCD8-RFP/UAS-mCD8-GFP;;	effector line
;LexAop-Stinger-GFP;;	effector line
;UAS-Cas9;;	effector line
;UAS-CD8-GFP;;	effector line
;UAS-Stinger-GFP;;	effector line
;Vas-Cas9	mutant
CS-TZ	wild type strain
ELAV-Gal4;Tub-Gal80^{ts};;	driver line
FoxP^{3955}	mutant
Integrase(x);;AttP2	mutant
w-;; D3/TM3, Sb	mutant
white-/-	mutant
WTB	wild type strain

Table 1: Complete list of the fly lines used in this study

2.2. *in-silico* sequences alignment

The transcript and protein sequences of the different FoxP isoforms were downloaded from https://flybase.org and aligned with *Clustal Omega* for multiple sequence alignment. The protein domains were analyzed with the *NCBI Conserved Domain Search* tool, and the stop codons were identified with *ExPASy Translate* tool (Fig. 1A).

2.3. Transgenics

We used CRISPR/Cas9 Homology Directed Repair (HDR) to edit the *FoxP* locus (Gratz et al., 2014) and generated t-RNA based vectors for producing multiple clustered regularly-interspaced (CRISPR) gRNAs from a single transcript (Port et al., 2016). We created a total of two driver lines (*FoxP-iB-Gal4* and *FoxP-LexA*), one mutant line (*FoxP-KO*) and one effector line (*UAS-t:gRNA(4xFoxP)*).

FoxP-iB-Gal4: To create an isoform-specific driver line, we inserted a Gal4 sequence into exon 8, which is specific to isoform B. Two 1 kb homology fragments were PCR-amplified (primers Hom1: fw 5'-GGGGGCGGCCGCCGTGGAAGGTAAAATGCCCCATATATG-3', rv 5'-GGGGCCGCGGCCCTCGTGTAAGGAAAGGTTCGTACGAATCGC-3'; primers Hom2: fw 5'-GGGGGGCGCGCCACAAGTGCTTTGTACGTTATG

AA-3′, rv 5′-GGGGGGTACCGGTCACTGAGTATCGTTAATGATC-3′) and digested with the appropriate restriction enzymes (Hom1: NotI and SacII, Hom2: AscI and KpnI) to be ligated in the pT-GEM(0) (Addgene plasmid # 62891; RRID:Addgene_62891) vector (Diao et al., 2015) which contained a Gal4 sequence and a 3xP3-RFP-SV40 sequence for selection of transformants. The gRNA sequences used are: sense 5′-CTTCGACGTACAAAGCACTTGTGTA-3′, and asense 5′-AAACTACACAAGTGCTTTGTACGTC-3′. They were annealed and cloned inside a pU6-gRNA (Addgene plasmid # 53062; RRID:Addgene_53062) vector (Shan et al., 2013), previously digested with BbsI restriction enzyme.

FoxP-LexA: To create a driver line that reflects expression of all *FoxP* isoforms, we inserted a LexA sequence into exon 3. Two 1 kb homology fragments were PCR-amplified (primers Hom1: fw 5′-GGGGGCGGCCGCCAGGAATGGCGGCATATGAGT-3′, rv 5′-GGGGCCGCGGCCCTCTATTACGGTAAGCGGACTCCGG-3′; primers Hom2: fw 5′-GGCCGGTACCATAGCATAGGCCGACCCATC-3′, rv 5′-GGCCACTAGTTCACATTCTCAACCCGCATAAAGC-3′) and digested with the appropriate

218 restriction enzymes (Hom1: NotI and SacII,
219 Hom2: KpnI and SpeI) to be ligated in the pT-
220 GEM(0) vector which contained a LexA
221 sequence and a 3xP3-RFP-SV40 sequence for
222 selection of transformants. The gRNA
223 sequences used are: sense 5'-
224 CTTCGGGTCGGCCTATGCTATTTA-3', asense 5'-
225 AAACTAAATAGCATAGGCCGACCC-3'. They were
226 annealed and were cloned inside a pU6-gRNA
227 vector previously digested with BbsI restriction
228 enzyme.

229 *FoxP-KO:* To prevent expression of any
230 isoform of the *FoxP* gene, we removed part of
231 exon 1, the complete exon 2 and part of exon
232 3. Two 1 kb homology fragments were PCR-
233 amplified (primers Hom1: fw 5'-
234 GGGGCTAGCCAAAATAAGATGTGTCTGGTTTCC
235 TTG-3', rv 5'-
236 GGGCCGCGGGCATGGCGAACTCATCGTG-3',
237 primers Hom2: fw 5'-
238 GGGGACTAGTAGAGGGAAAGTTTTGCCGG-3', rv
239 5'-
240 GGGGCTGCAGTATGAAGGGACAGATTGTGCCG
241 G-3') and digested with the appropriate
242 restriction enzymes (Hom1: NheI and SacII,
243 Hom2: SpeI and PstI) to be ligated in the pHD-
244 DsRed-attP (Addgene plasmid # 51019;
245 RRID:Addgene_51019) vector which contains a
246 3xP3-DsRed sequence for selection of
247 transformants. The gRNA sequences used are:
248 gRNA1 sense 5'-

CTTCGCGGATGATAGTACTTCCGCA-3′, asense 5′-AAACTGCGGAAGTACTATCATCCGC-3′; gRNA2 sense 5′-CTTCGAAGGACGTGCCCGGAAGAGA-3′, asense 5′-AAACTCTCTTCCGGGCACGTCCTTC-3′. They were annealed and were cloned inside a pU6-gRNA vector previously digested with BbsI restriction enzyme.

UAS-t:gRNA(4xFoxP): To create a UAS isoform-unspecific conditional effector line we phosphorylated and annealed 3 sets of oligos (1. fw 5′-CGGCCCGGGTTCGATTCCCGGCCGATGCAGAGCATCGATGAATCCTCAAGTTTCAGAGCTATGCTGGAAAC-3′, rv 5′-GCTCGGATATGAACTCGGGCTGCACCAGCCGGGAATCGAACC-3′; 2. fw 5′-GCCCGAGTTCATATCCGAGCGTTTCAGAGCTATGCTGGAAAC-3′, rv 5′-ACGGCATATGCCATGAGCAATGCACCAGCCGGGAATCGAACC-3′; 3. fw 5′-TTGCTCATGGCATATGCCGTGTTTCAGAGCTATGCTGGAAAC-3′, rv 5′-ATTTTAACTTGCTATTTCTAGCTCTAAAACAACCATGTTCCGTATTCAGATGCACCAGCCGGGAATCGAACC-3′) that were cloned with a single Gibson Assembly reaction in a pCFD6 (Addgene plasmid # 73915; RRID: Addgene_73915) vector (Port and Bullock, 2016) which was previously digested with BbsI restriction enzyme.

After the constructs were created, they were injected into early embryos (;*Vas/Cas9;* for the *FoxP-iB-Gal4, FoxP-LexA* and *FoxP-KO* and *Integrase(x);;AttP2* for *UAS-t:gRNA(4xFoxP)).* The resulting transformants were crossed two times with the balanced flies *w-;; D3/TM3, Sb*.

2.4. Immunohistochemistry

Three to six days-old adults were fixated in 4% paraformaldehyde (PFA) at 4 °C for 2 hrs and dissected in 0.01% phosphate-buffered saline with Triton® X-100 detergent (PBST). For larval staining, 3rd instar larvae were selected, dissected in 0.01% PBST and fixated in 4% PFA at room temperature (RT) for 30 min. Clean brains were washed 3 times in 0.01% PBST for a total time of 45 min and then blocked with 10% normal goat serum (NGS) for 1 hr. Subsequently the brains were incubated with the appropriate primary antibody for 1-2 nights at 4 °C (Table 2). After 3 washing steps of 15 min each, the brains were incubated with the secondary antibody (Table 3) for 5-7 hrs at RT. After an additional 15 min washing step, the brains were placed on glass microscope slides and mounted with the antifade mounting medium Vectashield® (Vector Laboratories, Burlingame, CA).

Antigen	Host	Dilution	Incubation	Source	RRID
Chaoptin-11	mouse	1:500	1 night	DSHB	AB_528161
ChAT	mouse	1:250	1 night	DSHB	AB_528122
ELAV	rat	1:100	1 night	DSHB	AB_528218
FoxP	guinea pig	1:200	2 nights	Lawton et al., 2014	/
GABA	rabbit	1:250	2 nights	GeneTex	AB_2037030
nc82	mouse	1:500	1 night	DSHB	AB_2314866
p-SMAD1/5	rabbit	1:250	2 nights	Cell Signaling Technology	AB_491015
REPO	mouse	1:500	1 night	DSHB	AB_528448
TH	rabbit	1:500	1 night	Millipore	AB_390204

Table 2. Complete list of the primary antibodies used in this study

Antigen	Host	Dilution	Incubation	Source	RRID
Anti-guinea pig Cy™3	goat	1:200	7 hours	Jackson ImmunoResearch	AB_2337423
Alexa-Fluor-Anti-mouse 555	goat	1:250	5 hours	ThermoFisher Scientific	AB_2535844
Alexa-Fluor-Anti-rabbit 555	goat	1:250	5 hours	ThermoFisher Scientific	AB_2535849
Alexa-Fluor-Anti-rat 555	goat	1:250	5 hours	ThermoFisher Scientific	AB_2535855

Table 3: Complete list of the secondary antibodies used in this study

313 ## 2.5. Image acquisition and analysis

314 All images were acquired with a Leica
315 SP8 confocal microscope (RRID: SCR_018169),
316 images were scanned at a frame size of
317 1024x1024 pixels at 200 or 100 Hz. The
318 objectives were 20x dry and 20x/40x/60x oil
319 immersion. Images were processed with
320 ImageJ software (National Institutes of Health,
321 Maryland, USA; RRID: SCR_003070) (Rueden et
322 al., 2017), only general adjustments to color,
323 contrast, and brightness were made. The cell
324 counting was performed with IMARIS 9.0
325 (Oxford instruments, UK) software on *UAS-*
326 *Stinger-GFP* stacks, using the tool for spots
327 counting. For the *FoxP-iB-Gal4/FoxP-LexA* count
328 (Fig. 4B), five brains were counted for each
329 genotype at both larval (3rd instar) and adult (2-
330 3 days old) stages. The colocalization analysis
331 was performed with the ImageJ *Colocalization*
332 *Threshold* tool (Tony Collins and Daniel James
333 White) (Fig 5B). The 3D rendering (Fig. 12B) was
334 performed with IMARIS 9.0 software on the
335 *Drosophila* standard brain from
336 https://www.virtualflybrain.org.

337 ## 2.6. RT-qPCR

338 The knockout efficiency was assessed
339 using RT-qPCR (see Figs. 1D, 4E). We extracted
340 RNA from 20 flies for each genotype (white$^-$,
341 heterozygous mutant and homozygous
342 mutant, both with a white$^-$ background),
343 following the TriFast™ protocol from peqlab (a

VWR company) (Catalog # 30-2010). The RNA was subsequently transcribed into cDNA using the OneStep RT-PCR Kit from QIAGEN (Catalog # 210212) with the following thermocycler program: 42 °C for 2 minutes, 4 °C pause until manual restart at 42 °C for 30 minutes, 95 °C for 3 minutes and finally 10 °C ∞. Subsequently we performed the qPCR. Primer sequences were identical to those used by (Mendoza et al., 2014). For the qPCR reaction we used a Bio-Rad CFX Connect Real-Time PCR Detection System thermocycler and the Bio-Rad CFX manager software to store and analyze the data. Every sample was run in triplicate in a 96-well plate in a total volume of 10 µl. The mixture contained 5 µl sybrGreen master mix (ORA™ qPCR Green ROX H Mix, 2X, from highQu, Catalog # QPD0201), 0.5 µl from each primer, 1 µl of 1:10 diluted cDNA and 3 µl H_2O. As reference, we used the housekeeping gene *rp49* (*ribosomal protein 49*), while as a negative control we used the same reaction mix without cDNA. The qPCR reaction program used was: 95 °C for 2 minutes, 95 °C for 10 seconds, 60 °C for 10 seconds, 65 °C for 30 seconds (from step 2 to 4 x 39 rounds), 95 °C for 10 seconds, and finally from 65 °C to 95 °C for + 0.5 °C / 5 s. The experiments were repeated 2 to 4 times.

2.7. Behavior

All behavioral experiments were performed in Buridan's paradigm (RRID:

375 SCR_006331) (Götz, 1980). In this experiment,
376 we analyzed both temporal components of
377 walking behavior (often subsumed under
378 'general locomotion') and spatial components
379 such as fixation of landmarks or the
380 straightness of the walking trajectory.
381 Buridan's paradigm (Fig. 6A) consists of a
382 round platform with a diameter of 117 mm
383 which is surrounded by a water-filled moat.
384 The platform is situated at the bottom of a
385 uniformly illuminated white cylinder, 313 mm
386 in height and 293 mm in diameter (Colomb et
387 al., 2012). Two black stripes are placed on the
388 inside of the cylinder, opposite each other,
389 serving as the only visual cues for the flies. Two
390 days-old female flies were collected and their
391 wings were clipped under CO_2 anesthesia.
392 After one night recovery at 25°C they were
393 tested in Buridan's paradigm for 15 minutes
394 (doi.org/10.17504/protocols.io.c7vzn5). The
395 position of the fly is recorded by a camera
396 (Logitech Quickcam Pro 9000) connected to a
397 computer running our BuriTrack software
398 (http://buridan.sourceforge.net) The analysis
399 software CeTrAn (Colomb et al., 2012)
400 (https://github.com/jcolomb/CeTrAn) extracts
401 a variety of parameters from the sored
402 trajectories. From the parameters extracted by
403 CeTrAn, we used the temporal parameters
404 median speed, distance travelled, number of
405 walks and activitytime and the spatial

parameters stripe deviation and meander. It furthermore traces occupancy plots. For the experiment involving *Tub-Gal80^{ts}* (Fig. 8E-H; 11A-B), flies were raised at 18 °C, moved to 30 °C for 12 hrs (embryos) or 48 hrs (pupae and adults) and subsequently left at 25 °C for the rest of the development (embryos and pupae) or overnight for recovery (adults) before testing.

2.8. Statistical analysis

All graphs were created and statistical analysis was performed using GraphPad Prism 6 (GraphPad Software, Inc., California, USA; RRID: SCR_002798) software and included unpaired (two-tailed) Student's t-test or one way ANOVA followed by Tukey's post hoc test. Alpha values were set to 0.5% (Benjamin et al., 2018).

The initial behavioral experiments (Fig. 6) were carried out with a sample size which, from experience, would be sufficient to detect medium to large effects, i.e., N~20. We then used these results to perform a power analysis for the subsequent experiments. We found that effect sizes such as those exhibited in the speed, meander or stripe fixation parameters required a sample size of up to 18 to reach 80% statistical power at an alpha of 0.5% (Benjamin et al., 2018), while effects such as those in the activity time parameter would require up to 100 flies. We corroborated these analyses with

Bayesian analyses, where the activity time parameter yielded a Bayes factor below one, while the other effects yielded Bayes factor values beyond 100. Therefore, we set the target sample size for all subsequent Buridan experiments to 18 and $p<0.005$ was considered significant. Data are expressed as averages ± SEM or averages ± SD, and each case is indicated in the legend of each figure.

2.9. Data deposition

All raw data is publicly accessible with an Attribution 4.0 International (CC BY 4.0) license. Data sources are referenced in the text.

3. Results

3.1. *FoxP-iB* expression in the *Drosophila* brain

The *FoxP* transcription factor binds DNA with the forkhead (FH) box domain (Fig. 1A, yellow boxes; raw data deposited at 10.6084/m9.figshare.12607700). The gene consists of 7 introns and 8 exons. The FH box is split into different segments spanning exons 6, 7 and 8. The last two exons (7 and 8) are subjected to alternative splicing, leading to two different protein isoforms: isoform A (*FoxP-iA*), which results from splicing exon 6 to exon 7, and isoform B (*FoxP-iB*) where instead exon 8 is

spliced to exon 6. A third, intron-retention isoform is transcribed by failing to splice the intron between exon 6 and 7 out (*FoxP-iIR*). While the first two isoforms contain a complete and putatively functioning FH box (with 10 amino acids different between the two; Fig.1A, dashed box), the putative FoxP-iIR FH box appears to be truncated due to a stop codon in the intron sequence (Fig. 1A, red line), rendering the transcription factor function of this isoform more than questionable. Of the three FoxP isoforms, *FoxP-iB* was most directly associated with the learning phenotype discovered by (Mendoza et al., 2014). Therefore, we inserted the sequence of the yeast transcription factor Gal4 into exon 8, the exon which is exclusive to *FoxP-iB* (Fig. 1A). This insertion leads to the expression of the Gal4 transcription factor only in *FoxP-iB* positive cells. At the same time, the insertion also disrupts the FH box DNA binding domain of the *FoxP* gene, putatively preventing the FoxP protein to act as a transcription factor, effectively mutating the gene for this function.

Observing Gal4 expression with different green fluorescent proteins (GFPs) under control of the UAS promoter (to which Gal4 binds), revealed that *FoxP-iB* is expressed throughout the whole development of the fly, from embryo (data deposited at 10.6084/m9.figshare.12607652) to adult, in

both brain and ventral nerve cord (VNC) (Fig. 1B). Main expression domains in the neuropil comprise protocerebral bridge, gnathal ganglia (subesophageal zone), vest, saddle, noduli, and superior medial protocerebrum. GFP-positive cell body clusters could be found in the cortex of the central brain and around the optic lobes (Fig. 1B).

We next validated the expression pattern of our iB-specific driver line to the staining of an available isoform unspecific polyclonal antibody (Lawton et al., 2014). We observed complete colocalization of the driver line with the antibody staining in both larvae and adults, i.e., there were no GFP-positive cells that were not also labeled by the FoxP antibody (Fig. 1C). The cells only stained for the FoxP antibody and not for GFP are presumably cells expressing the other *FoxP* isoforms (*FoxP-iA* and *FoxP-iIR*, Fig. 4). Notably, in contrast to previous reports (DasGupta et al., 2014; Groschner et al., 2018) but consistent with (Castells-Nobau et al., 2019), we did not detect any *FoxP* expression in mushroom body neurons, neither with our driver line, nor with the antibody.

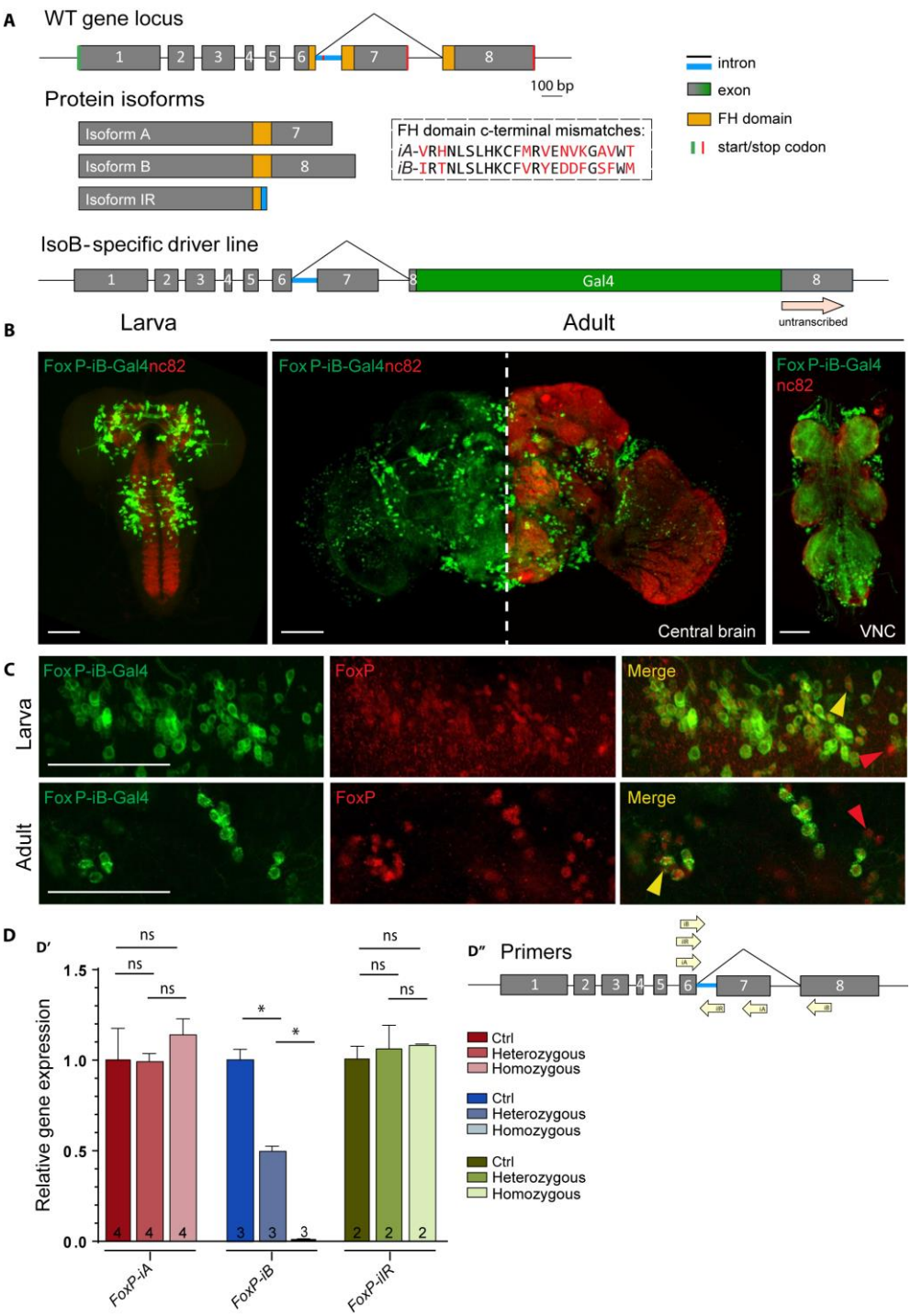

Fig. 1: *FoxP-iB expression in the* Drosophila *nervous system.*
(A) Schematic representation of the *FoxP* gene locus before (above) and after (below) insertion of a Gal4 sequence into exon 8. (B) *FoxP-iB-Gal4>CD8-GFP* expression pattern costained with nc82 in 3rd instar larvae, adult brain and adult VNC. (C) Driver line costained with a polyclonal FoxP antibody in larval and adult brain. The yellow arrowheads indicate colocalization, while the red ones indicate cells only positive for the antibody staining. (D') RT-qPCR for FoxP-iA, iB and IR on controls and hetero and homozygous *FoxP-iB-Gal4* mutant. (D") Primers used for the RT-qPCR. Data are expressed as means ± SEM. *p<0.005. Scale bars: 50 µm.

Postulating that our transgene disrupted expression of the *FoxP* gene, we measured mRNA levels of all three isoforms with RT-qPCR (Fig.1D). With one of the primers placed over the Gal4 insertion site, we observed approximately half the wild type *FoxP-iB* expression levels in heterozygous animals, while wild type *FoxP-iB* expression was essentially abolished in the homozygous transgenes. We did not observe any change in the other two isoforms. However, this disruption of the *FoxP-iB* isoform did not have an effect on the development of the *FoxP*-positive neurons, as both heterozygous and homozygous *FoxP-iB-Gal4* mutants showed the same number of GFP-labelled cell nuclei (data deposited at 10.6084/m9.figshare.12932705).

3.2. *FoxP-iB* is expressed in a variety of neurons, but not glia

With *FoxP* involved in learning and expression patterns suggesting neuronal expression (Fig. 1), we investigated whether the observed expression was exclusively neuronal, or if there were also *FoxP-iB* expressing glial cells. Therefore, we stained 3rd instar larva and adult brains with antibodies against ELAV (neuronal marker) and REPO (glial marker). At both developmental stages, the two stainings reveal exclusive *FoxP-iB*-mediated GFP colocalization with ELAV without any colocalization with REPO (Fig. 2A-B; raw

562 data deposited at
563 10.6084/m9.figshare.12607706), suggesting
564 that *FoxP-iB* is expressed exclusively in
565 neurons. These data are consistent with
566 results published previously (Castells-Nobau et
567 al., 2019; Lawton, 2014), validating the
568 methods employed here.

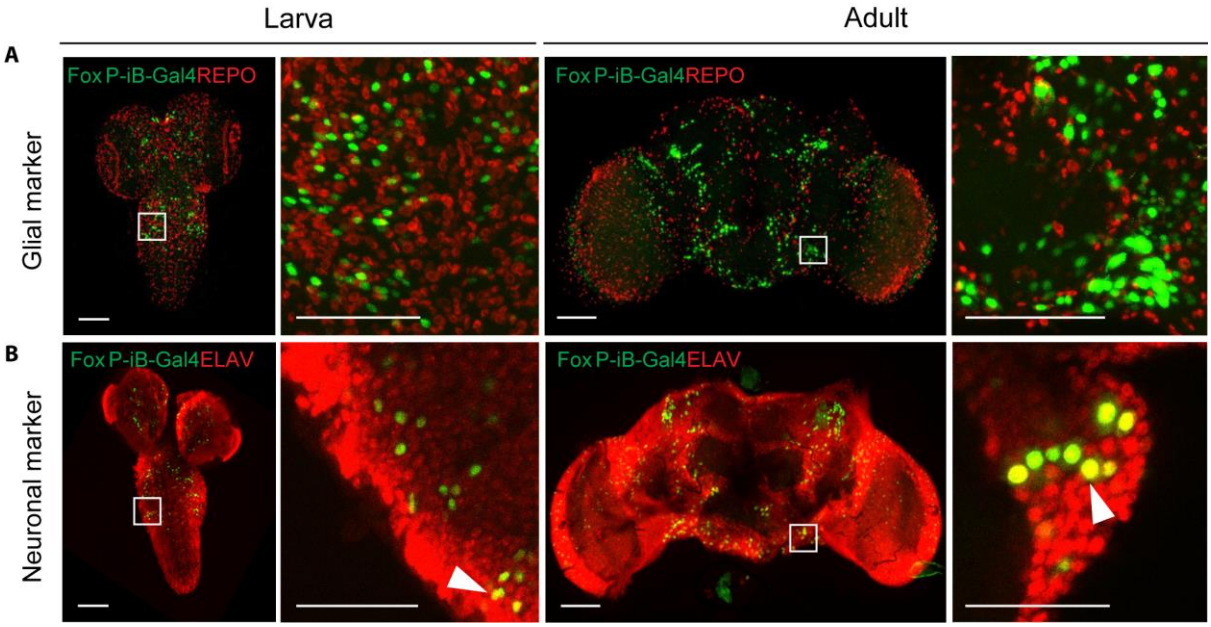

569

570 **Fig. 2**: *Only neurons, not glia, are expressing* FoxP-iB *in the* Drosophila *brain.*
571 Immunohistochemistry on *FoxP-iB-Gal4>Stinger-GFP* flies with REPO (glia, A) and ELAV (neurons, B)
572 markers. Note the lack of colocalization of *FoxP-iB* driven GFP with the glial marker in both 3rd
573 instar larvae and adult brains (A). In contrast, exclusive colocalization of *FoxP*-driven GFP with the
574 neuronal marker was observed in both developmental stages (white arrowheads indicate typical
575 examples). Scale bars: 50 µm.

576 We next investigated in more detail the
577 types of neurons in which *FoxP-iB* is expressed.
578 Using a variety of antibodies (Fig. 3; raw data
579 deposited at 10.6084/m9.figshare.12607712)
580 used as markers for different neuronal cell
581 types we detected *FoxP-iB* expression in most
582 of the cell types investigated: extensive
583 colocalization was observed with p-SMAD1/5 (a

motorneuron marker) in the VNC but not in the central brain (CB) (Fig. 3A). Some *FoxP-iB* neurons were positive for ChAT (cholinergic) or GABA (inhibitory) both in the VNC and in the CB (Fig. 3B-C). Finally, a few *FoxP-iB* positive neurons were found to colocalize with Tyrosine hydroxylase (dopaminergic neurons) in the CB only (Fig. 3D). These data are consistent with the study performed by *(Schatton et al., 2018)* in honeybees where they found colocalization between AmFoxP positive neurons and GABAergic, cholinergic and monoaminergic markers. No colocalization was instead found in photoreceptor cells stained with Chaoptin (data deposited at 10.6084/m9.figshare.12607643), a marker for photoreceptor cells (Pollock et al., 1990).

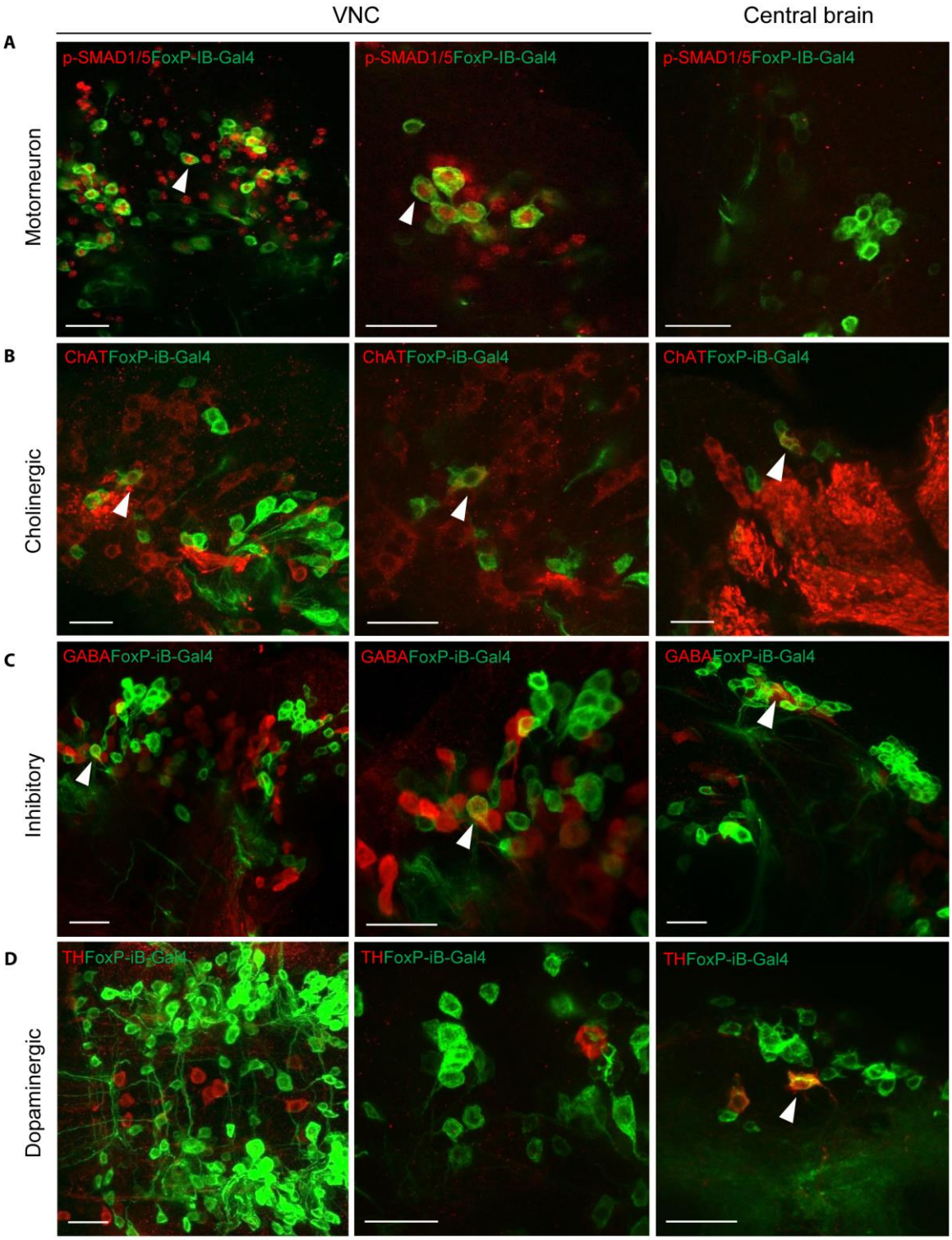

601

602 **Fig. 3**: FoxP-iB *is expressed in various types of neurons.*
603 Immunohistochemistry on *FoxP-iB-Gal4>CD8-GFP* flies using different antibodies. (A) Some of
604 the *FoxP-iB* positive neurons colocalize with p-SMAD1/5 in the VNC but not in the central
605 brain. (B-C) *FoxP-iB* neurons positive for ChAT or GABA have been found in both the VNC and
606 CB. (D) Only few *FoxP-iB* neurons colocalize with TH and only in the CB. White arrowheads
607 indicate examples of colocalization. Scale bars 25 µm.

3.3. *FoxP-iB* is expressed in a subset of *FoxP*-expressing neurons

As the antibody staining against the FoxP protein indicated more cells expressing FoxP than our *FoxP-iB*-specific driver line was reporting (Fig. 1B), we created a second driver line, designed to drive expression in all FoxP cells, irrespective of isoform. We inserted a sequence for the bacterial LexA (Szüts and Bienz, 2000) transcription factor into exon 3 (Fig. 4A; raw data deposited at 10.6084/m9.figshare.12607730). Comparing *Stinger-GFP* expression from each driver line revealed a more expansive pattern for the isoform-unspecific driver (Fig. 4B), one that matches very well with the FoxP antibody staining (Fig. 1B). This visual impression was corroborated by a quantification of stained nuclei comparing between both drivers (Fig. 4C). This quantification allowed us to trace the proliferation of FoxP cells from around 500 in 3rd instar larvae to around 1800 in three days-old adults. In contrast, there are only about 300 cells expressing *FoxP-iB* in the 3rd larval instar and only around 1300 in three days-old adults. We noticed that the largest differences in terms of cell number between *FoxP-LexA* and *FoxP-iB-Gal4* flies (both larvae and adults) were found in the CB, while the VNC numbers differed considerably less. Taken together, in 3rd instar larvae and in three days-old adults,

639 66% and 65%, respectively, of the total number
640 of *FoxP* neurons in the *Drosophila* nervous
641 system express *FoxP-iB*. As with our previous
642 insertion, also this one was expected to disrupt
643 expression of the *FoxP* gene. To investigate the
644 extent of this disruption on the mRNA level, we
645 again performed RT-qPCR. As expected, this
646 insertion affected all isoforms. In heterozygous
647 flies, the expression level was increased, while
648 in homozygous flies it was decreased (Fig. 4E).
649 It is important to note that the reverse primers
650 for these isoforms were chosen to target
651 sequences downstream of the insertion site
652 (see Fig. 1A).

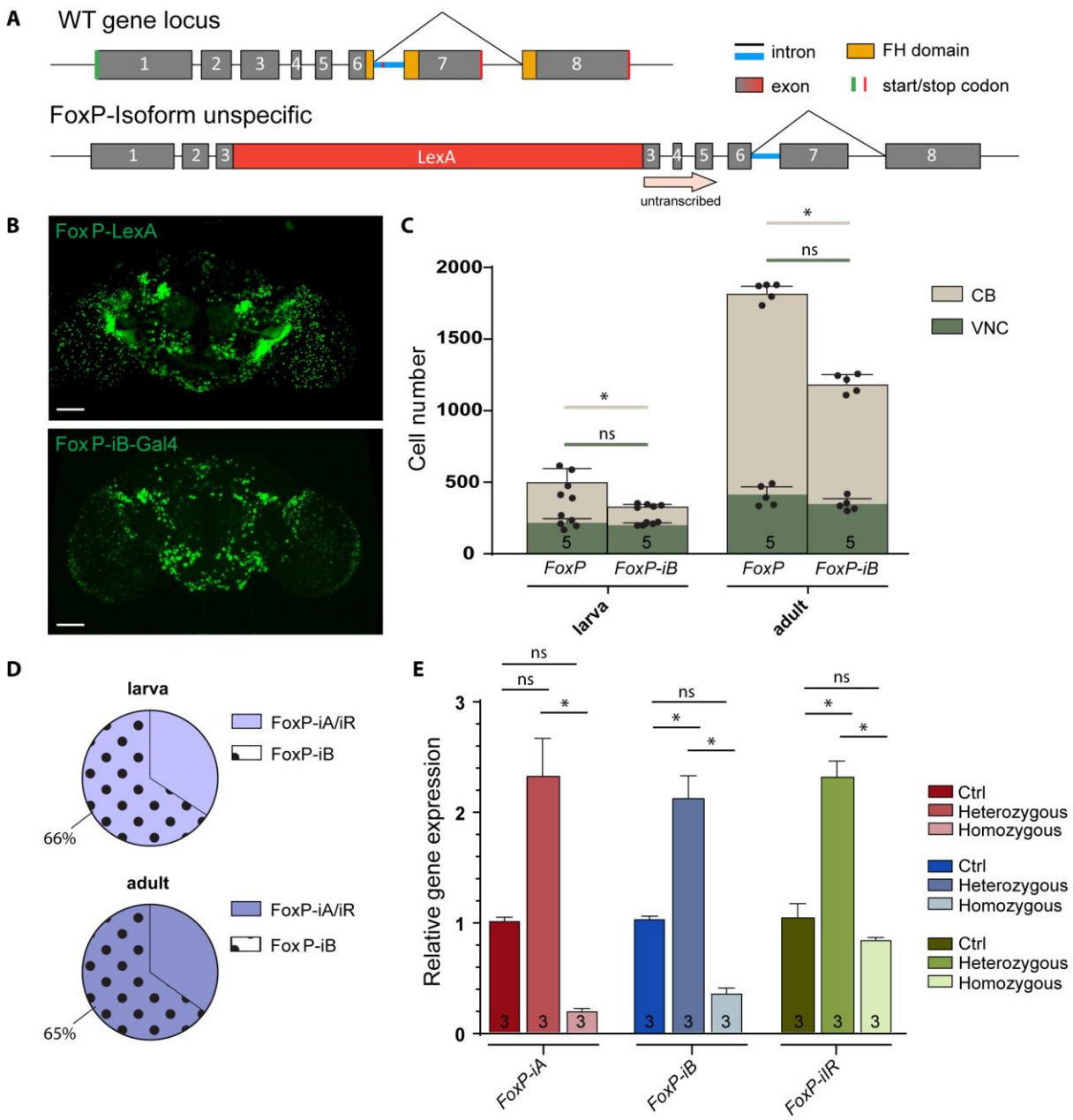

Fig. 4: FoxP-iB *is expressed in a subset of FoxP-expressing neurons*.
(A) Schematic representation of the FoxP gene locus after LexA insertion. This is an isoform unspecific construct with the insertion of a LexA sequence in exon 3. (B) Expression pattern of *FoxP-LexA* and *FoxP-iB-Gal4* driving *Stinger-GFP*. (C) Cell counting performed with IMARIS on *FoxP-LexA* and *FoxP-iB-Gal4>Stinger-GFP* (3rd instar larvae and 3 days-old adults) in both CB and VNC. (D) Pie charts that summarize the results from (C). (E) RT-qPCR on FoxP-LexA flies (control, hetero- and homozygous flies). Data are expressed as means ± SD in (C) and as means ± SEM in (E). *p<0.005. Scale bars: 50 µm.

In order to directly compare the expression patterns of our two driver lines, we used them to drive reporter genes fluorescing

665 at different wavelengths (i.e., *LexAop-RFP;UAS-*
666 *CD8-GFP*) and analyzed their patterns in adults
667 (Fig. 5; raw data deposited at
668 10.6084/m9.figshare.12607763). In this way,
669 we labeled all *FoxP*-expressing neurons red
670 and neurons that specifically expressed *FoxP-*
671 *iB* green. We used the "Colocalization
672 Threshold" tool from ImageJ, which computes
673 false colors to enhance the comparison
674 between the two driver lines and let the
675 differences stand out (see M&M). The other
676 two isoforms are expressed in additional areas
677 (the vast majority of the antennal lobe, the
678 lobula, the fan shaped body and the posterior
679 ventrolateral protocerebrum) compared to
680 *FoxP-iB* expression (Fig. 5A, red arrowheads;
681 Fig. 5B, blue areas).

682 We also crossed this *FoxP-LexA* line with
683 *LexAop-RFP-UAS-CD8-GFP* and *Tdc2-Gal4* to
684 investigate any potential tyraminergic or
685 octopaminergic *FoxP* neurons, but despite a
686 close proximity between the two cell types, no
687 colocalization was found (data deposited at
688 10.6084/m9.figshare.12607670).

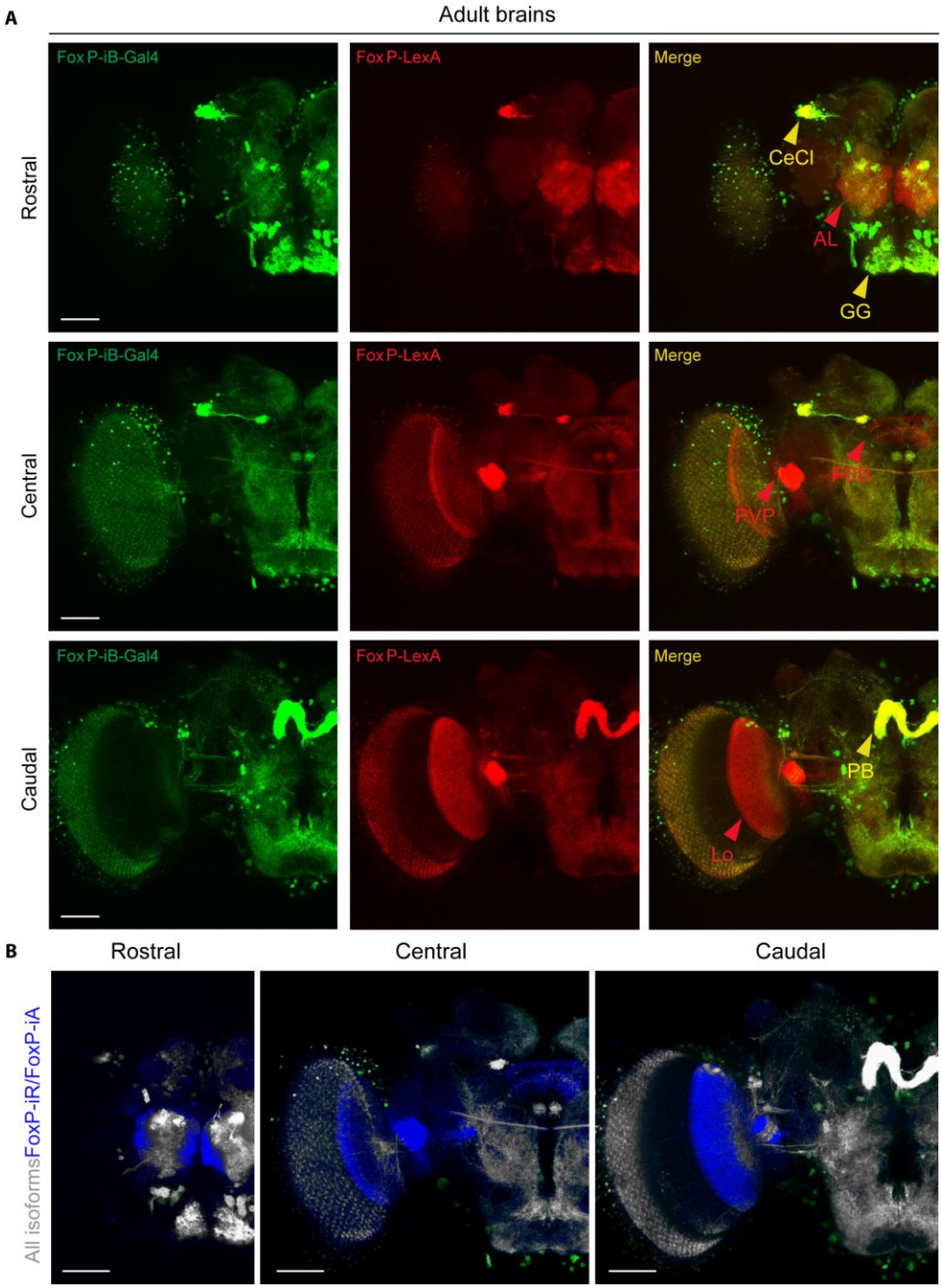

Fig. 5: FoxP-iB expression pattern compared to the one of FoxP. (A-B) Confocal images of adult brains that express *FoxP-iB-Gal4>CD8-GFP* (green) and *FoxP-LexA>CD8-RFP* (red) together. The image shows in green the areas that express FoxP-iB, in red the total FoxP expression in the Drosophila brain (AL: antennal lobe, PVP: posterior ventrolateral protocerebrum, FSB: fan shaped body, Lo: lobula) and in yellow the areas that are stained by both constructs (cecl: cell cluster, GG: gnathal ganglion, PCB: protocerebral bridge). Scale bars: 50 µm.

3.4. *FoxP-iB* knockout flies show a multitude of behavioral abnormalities

Mutations in the *FoxP* gene do not only affect operant self-learning, for instance, different alleles also affect flight performance and other locomotion behaviors to different degrees (Castells-Nobau et al., 2019; Lawton et al., 2014; Mendoza et al., 2014). Because of the *FoxP* pleiotropy affecting various innate motor behaviors independently from motor learning, we turned to Buridan's paradigm (Colomb et al., 2012; Götz, 1980) as a powerful tool to measure several locomotor variables. Buridan's paradigm allows us to test a broad panel of behavioral parameters covering temporal parameters such as speed or general activity time and spatial parameters such as the straightness of a fly's trajectory (meander) or the degree to which the animal is heading towards one of the two vertical landmarks (stripe fixation; Fig. 6A).

With our insertions constituting novel alleles impairing *FoxP* expression (Figs. 1, 4), we started by testing the heterozygous and homozygous driver strains without any effectors.

Consistent with previous findings of impaired locomotor behavior in *FoxP* manipulated flies (Castells-Nobau et al., 2019; Lawton et al., 2014; Mendoza et al., 2014) and

727 the qPCR results showing reduced *FoxP*
728 expression (Fig. 1D), our *FoxP-iB-Gal4* insertion
729 shows abnormalities in Buridan's paradigm
730 both in temporal and in spatial parameters
731 (Fig. 6; raw data deposited at
732 10.6084/m9.figshare.12607769). While the
733 homozygous flies walked more slowly, spent
734 more time at rest and fixated the stripes less
735 strongly than wild type control flies,
736 heterozygous flies only differed from wild type
737 flies in their stripe fixation (Fig. 6C). With
738 different effect sizes in each parameter, we
739 selected two representative parameters each
740 for the temporal and the spatial domain,
741 respectively, for comparison of all subsequent
742 lines: walking speed, activity time, meander
743 and stripe fixation.

744 Because our insertion is located in the
745 same exon as the insertion in the $FoxP^{3955}$
746 mutant, we tested the $FoxP^{3955}$ mutant flies in
747 Buridan's paradigm and found changes in
748 several temporal parameters, similar to those
749 observed in our driver line (Fig. 6D). However,
750 stripe fixation appears normal in these flies.
751 Thus, besides the deficits in operant self-
752 learning and flight performance as reported
753 previously (Mendoza et al., 2014), the $FoxP^{3955}$
754 mutant flies are also deficient in several
755 temporal parameters of walking behavior in
756 Buridan's paradigm. This walking phenotype is
757 consistent with previous findings of walking

deficits associated with *FoxP* manipulations (Castells-Nobau et al., 2019; Lawton et al., 2014), but was not detected in a previous publication where tests for walking deficits had been performed (DasGupta et al., 2014).

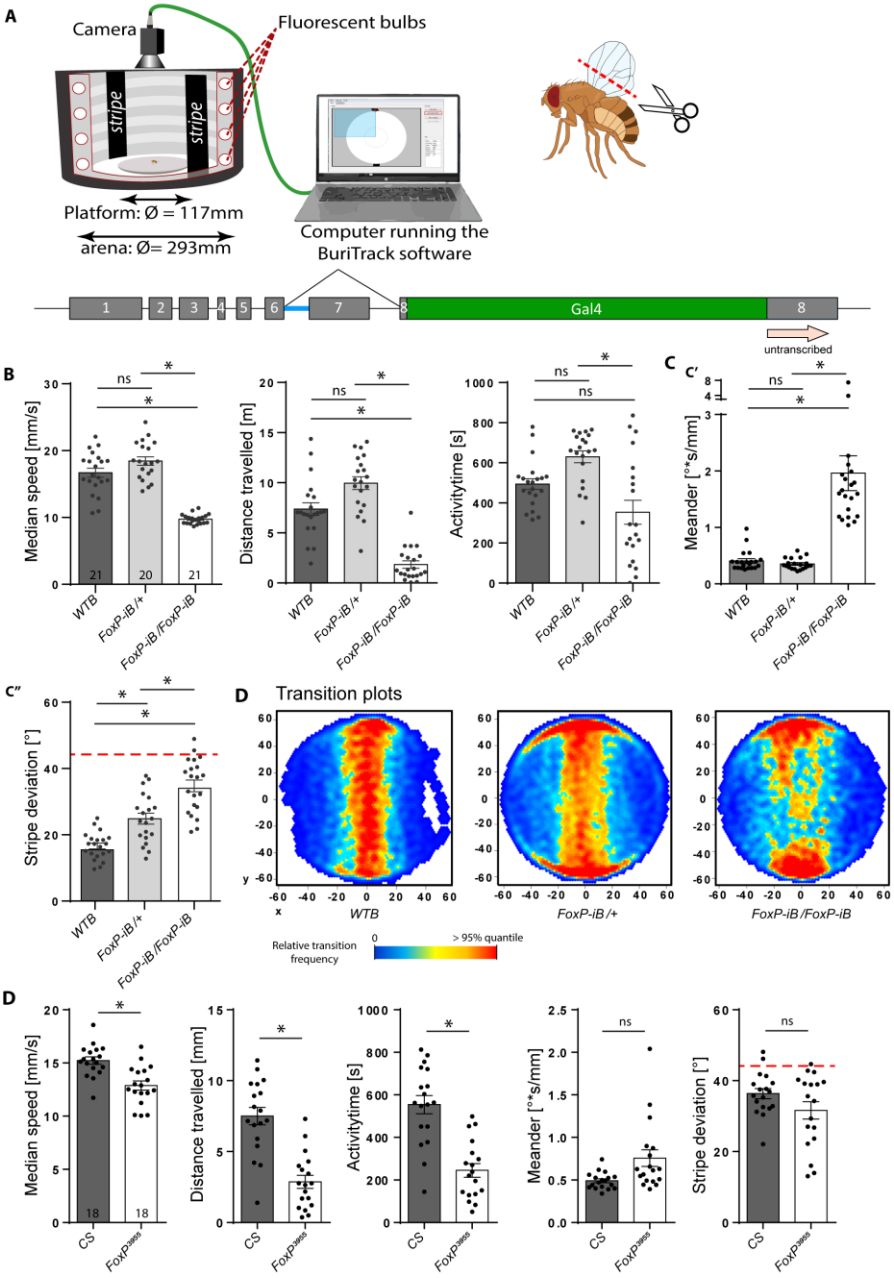

Fig. 6: FoxP-iB *mutant flies are impaired in several parameters in Buridan's paradigm*. (A) Schematic of Buridan's paradigm. A fly with shortened wings is put in the center of a platform inside a circular arena with two opposing black stripes on the walls. A camera records the position of the fly and the BuriTrack software stores the position data for later analysis with CeTrAn. (B) Temporal parameters. Median speed denotes the instantaneous speed when a fly is walking. Activity time denotes the time spent walking. Distance traveled measures the distance covered by the fly during the experiment. (C) Spatial parameters. Stripe deviation measures the angular deviation from heading towards the center of the stripe to which the fly is oriented. Red dashed line indicates angular stripe deviation of a random walk. The transition plots show the distribution of the platform locations that the flies transitioned through. Meander is a measure for the straightness of a fly's trajectory. *p<0.005.

3.5. Knocking out all *FoxP* isoforms has similar effects as *FoxP-iB* knockout

With such dramatic motor alterations when only *FoxP-iB*, which is expressed in about 65% of all *FoxP*-positive neurons (Fig. 4), is removed (Fig. 6), it is interesting to study the effects of removing the remaining isoforms for a complete *FoxP* knockout. To avoid unwanted potential side-effects of expressing a different protein in its stead, we created a third fly line where the entire second exon is removed together with parts of exons 1 and 3. We validated this mutant with the polyclonal antibody we used before (Fig. 1). While the antibody detected the FoxP gene product in control flies, there was no signal in our homozygous knock-out flies (Fig. 7A, B; raw data deposited at 10.6084/m9.figshare.12607796).

Analogous to the behavioral characterization in the *FoxP-iB* insertion line, we tested both heterozygous and homozygous *FoxP-KO* deletion mutants in Buridan's paradigm (Fig. 7C-F). The results of this experiment closely resemble the ones from the *FoxP-iB*-Gal4 insertion line, with homozygous mutants being both significantly less active (Fig. 7C) and fixating the stripes less strongly than the heterozygous mutants and the wild type controls (Fig. 7D, E). For this allele, the heterozygous *FoxP-KO* mutants show

807 higher values for all temporal parameters
808 compared to the wild type controls, while there
809 is no difference in stripe deviation. This trend
810 was already observed in *FoxP-iB* mutants but
811 failed to reach statistical significance. Thus, the
812 *FoxP-KO* allele exhibits differential dominance,
813 with recessive modes of inheritance in some
814 traits and, e.g., overdominance in others. A
815 direct comparison of the data from the two
816 homozygous alleles (*FoxP-iB* and *FoxP-KO*)
817 showed no significant differences (Fig. 7F).
818 Thus, removing the other *FoxP* isoforms had
819 few effects beyond the consequences of
820 removing only *FoxP-iB* alone.

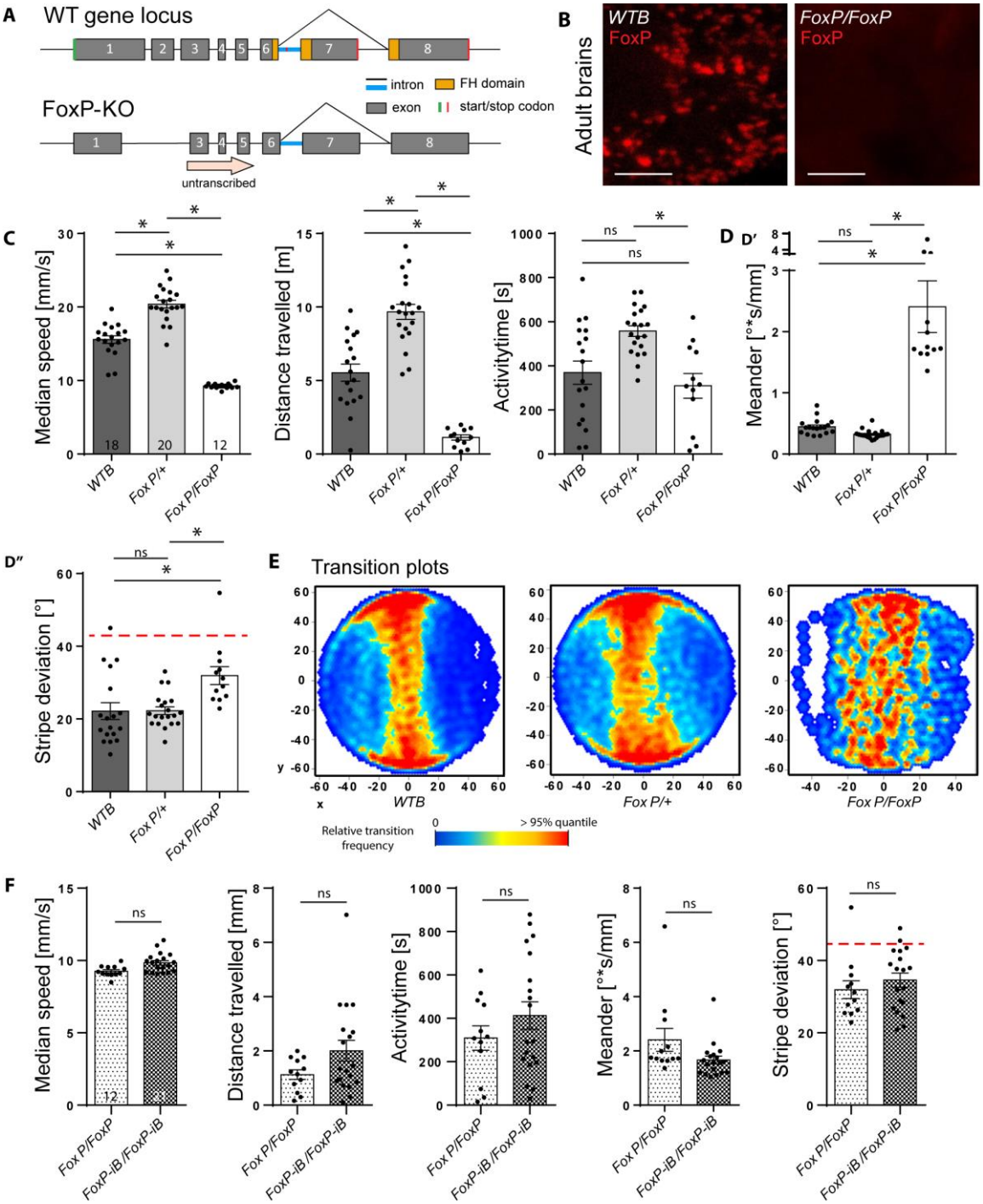

Fig. 7: *Deleting the entire* FoxP *gene has similar consequences in Buridan's paradigm as deleting only* FoxP-iB.

(A) Schematic representation of the deletion (*FoxP-KO*) and the wild type (*WT*) gene locus. (B) Immunohistochemistry staining for the FoxP gene product in wild type and FoxP-KO mutant brains. (C) Temporal parameters. See Fig. 7 and M&M for definitions. Note the overdominance of the heterozygous *FoxP-KO* flies. Stripe deviation (D) and transition plots (E) show weaker stripe fixation of homozygous FoxP-KO flies. (F) Comparing *FoxP-KO* and *FoxP-iB* flies reveal only a small difference in walking speed. *p<0.005. Scale bars: 25 µm.

3.6. Conditional *FoxP* knock-out (*FoxP-cKO*)

Given the patchy expression pattern of *FoxP* in the fly's nervous system (Figs. 1-5) and the grave consequences for behavior in Buridan's paradigm if it is manipulated (Figs. 6, 7), we sought to investigate when and where *FoxP* is required for normal walking behavior. To this end, we designed a fourth fly strain which carries a UAS-controlled effector (Fig. 8A; raw data deposited at 10.6084/m9.figshare.12607805). The four guide RNAs (gRNA) each target a different section of the *FoxP* gene (see M&M). If expressed together with the endonuclease Cas9, this effector efficiently mutates the targeted gene (Port and Bullock, 2016; Xie et al., 2015). We validated this approach by driving both our gRNAs as well as Cas9 using the pan-neuronal *elav-Gal4* driver and monitoring *FoxP* expression with the FoxP antibody used before (Fig. 8B). Flies with this pan-neuronal excision of the *FoxP* gene (*FoxP-cKO*) were also tested in Buridan's paradigm and showed even more severe impairments than flies homozygous for a constitutive deletion of the gene (Fig. 8C). In fact, the mutated flies walked so little, that analysis of spatial parameters was not meaningful (Fig. 8D). To allow for temporal control of transgene expression, we also validated the use of the temperature-sensitive suppressor of Gal4,

Gal80^{ts} (Fig. 8E). The constitutively expressed Gal80^{ts} prevents Gal4 from activating transcription of the UAS-controlled transgenes until the temperature is shifted from 18 °C to 30 °C, at which point the repressor becomes inactivated and Gal4-mediated transcription commences (McGuire et al., 2004, 2003). Using this system to drive gRNA/Cas9 expression for 12 hours in the embryo phenocopies both the mutant and the conditional phenotypes not only on the protein (Fig. 8F), but also on the behavioral level (Fig. 8G, H). In both experiments, the effects of the manipulations were so severe, that it was not possible to reach the target sample size of 18.

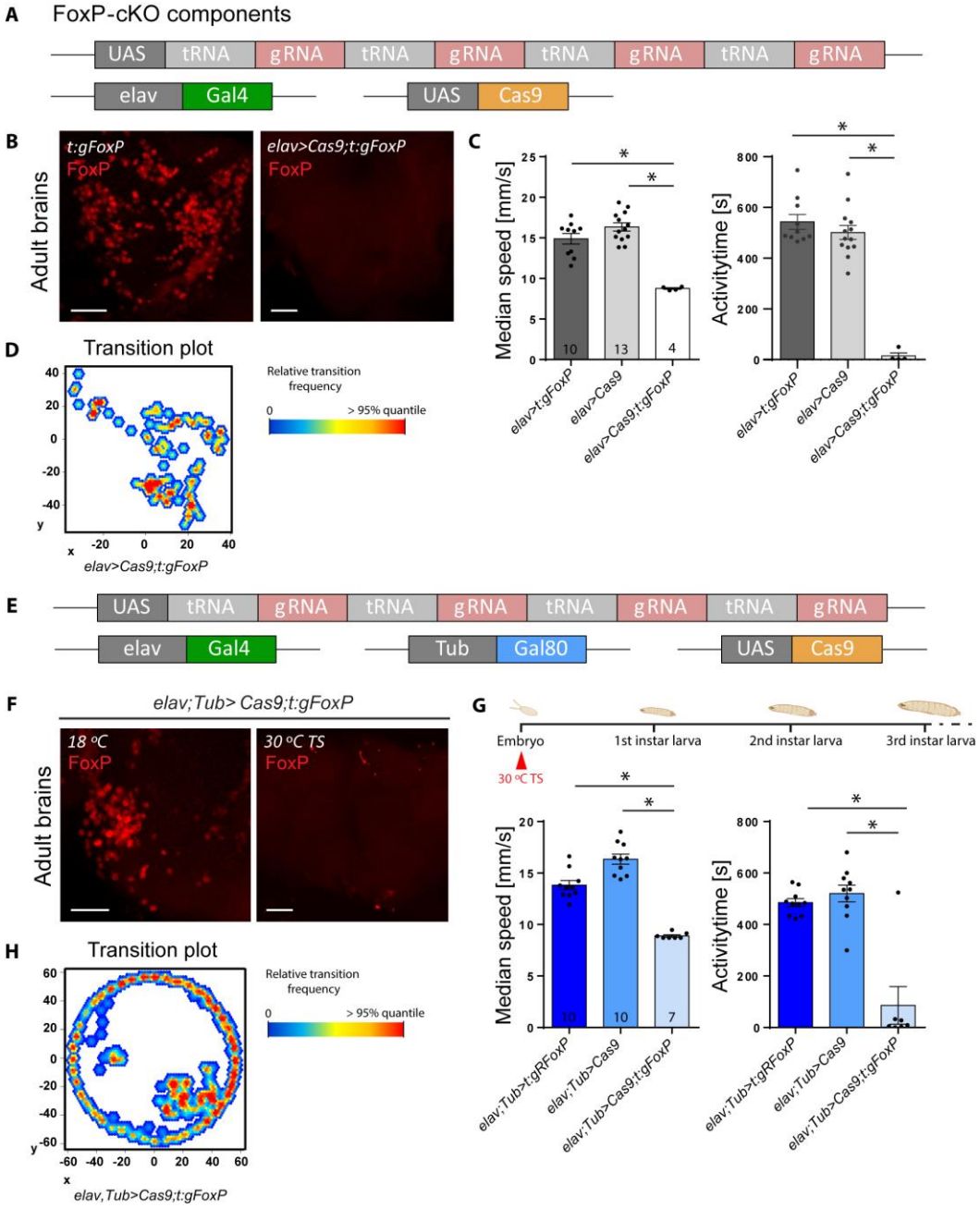

Fig. 8: *Conditional* FoxP *gene knock-out mimics mutant phenotype*.
(A) Construct schematic of the effector (UAS) line we created, together with the *elav* driver line and *Cas9* effector. (B) Immunohistochemistry on adult brains of the effector control line (left), and of the experimental cross (right). Driving expression of our gRNA construct with *elav-Gal4* leads to a highly efficient *FoxP* gene knock-out. (C) This knock-out is also validated in Buridan's paradigm, where the experimental flies show strongly reduced locomotor activity. (D) Transition plot showing the reduced activity of *FoxP-cKO* flies. (E) Schematic of the used transgenic elements. Gal80^{ts} inhibits Gal4 under 30 °C. (F) Induction of panneural gRNA expression in the embryo eliminates FoxP expression as tested with a FoxP antibody (right) compared to uninduced controls (left). (G-H) Inducing panneural gRNA expression in the embryo also leads to similar locomotor defects as observed in mutants and in flies expressing the gRNAs without temporal control. *p<0.005. Scale bars: 25 µm

3.7. Conditional *FoxP-KO*: brain regions and neuron types

Recently, Linneweber *et al. (2020)* described the consequences of silencing dorsal cluster neurons (DCNs) on stripe fixation behavior in Buridan's paradigm. The *FoxP-iB* expression pattern suggests that at least some of these DCNs express FoxP (Fig. 1). Comparing our isoform-unspecific *FoxP-LexA* expression pattern with that of the *atonal-Gal4* line used to drive expression in DCNs (Hassan et al., 2000), we observed substantial overlap (Fig. 9A; raw data deposited at 10.6084/m9.figshare.12607811). Therefore, we use *ato-Gal4* to excise the *FoxP* gene specifically in DCNs. Interestingly, this manipulation did not have any effect on the flies' behavior in Buridan's paradigm (Fig. 9B).

The insect mushroom-bodies (MBs) are not only known as a center for olfactory learning and memory (Dolan et al., 2018; Felsenberg et al., 2018; König et al., 2019; Lyutova et al., 2019; Thum and Gerber, 2019; Turrel et al., 2018; e.g., Warth Pérez Arias et al., 2020; Widmer et al., 2018), they are also involved in the temporal and spatial control of locomotor activity (Besson and Martin, 2005; Helfrich-Förster et al., 2002; Lark et al., 2017; Lebreton and Martin, 2009; Mabuchi et al., 2016; Manjila et al., 2019; e.g., Martin et al., 1998; Serway et al., 2009; Sun et al., 2018; Xiong

921 et al., 2010). In addition, (Castells-Nobau et al.,
922 2019) found a subtle structural phenotype in a
923 sub-section of the MBs without detectable *FoxP*
924 expression in the MB Kenyon cells themselves.
925 Finally, there are two reports that expressing
926 anti-*FoxP* RNAi constructs exclusively in the
927 MBs can have behavioral effects (DasGupta et
928 al., 2014; Groschner et al., 2018). For these
929 reasons, despite neither (Castells-Nobau et al.,
930 2019) nor us being able to detect any FoxP
931 expression in the MBs, we deleted the *FoxP*
932 gene from MB Kenyon cells using the *ok107-*
933 *Gal4* driver and tested the flies in Buridan's
934 paradigm. We did not detect any differences to
935 control flies in these experiments (Fig. 9C).

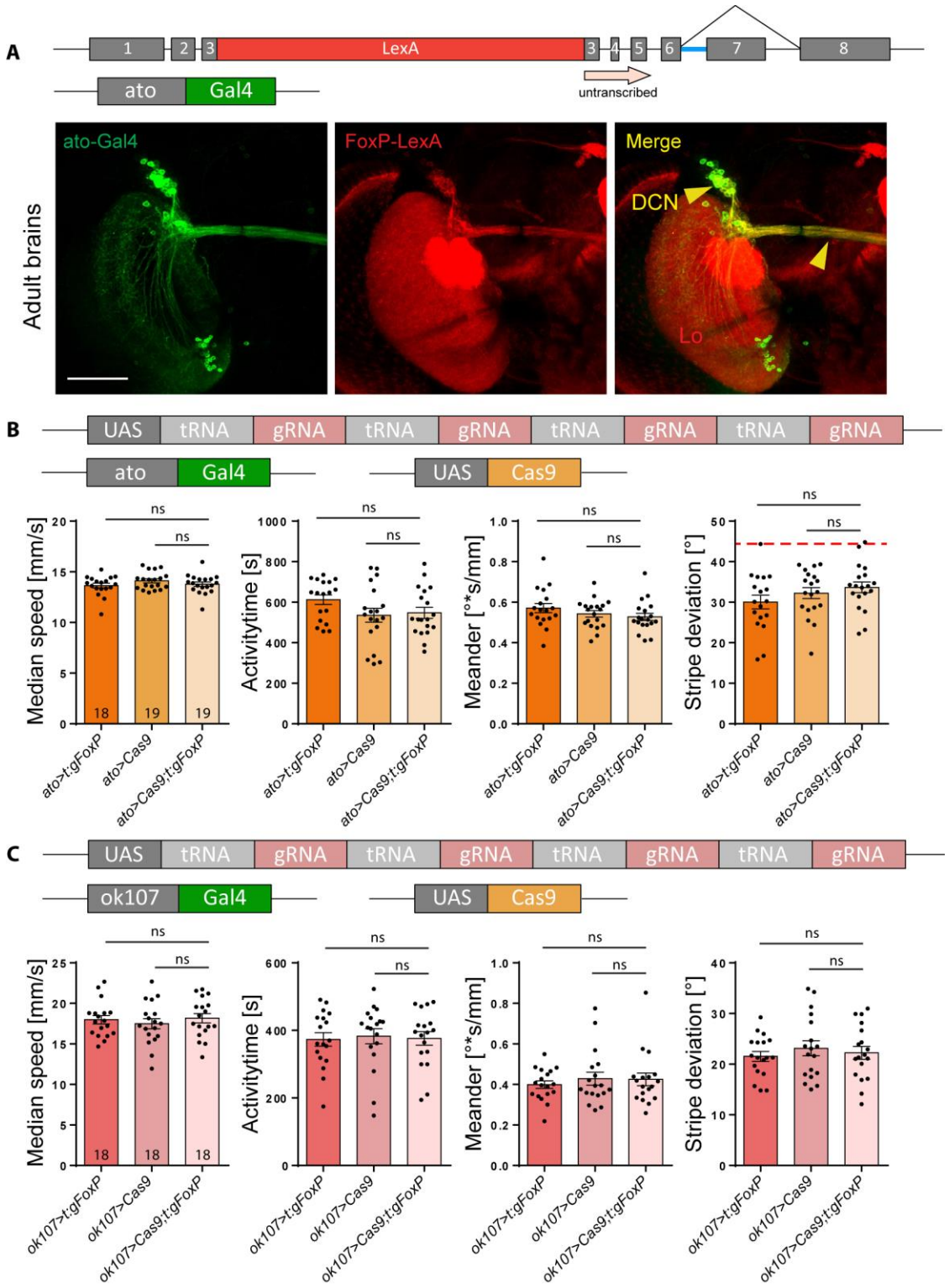

Fig. 9: *Conditional* FoxP-KO *shows no effect in dorsal cluster neurons or mushroom bodies*. (A) Immunohistochemistry showing *FoxP-LexA* expression in the adult brain compared to the expression of the *ato-Gal4* driver. DCN: dorsal cluster neurons, Lo: lobula, Scale bars: 50 µm. (B) Temporal and spatial parameters from Buridan's experiment show no effects of knocking out the *FoxP* gene in dorsal cluster neurons using the *ato-Gal4* driver. (C) Knocking out the *FoxP* gene in the mushroom bodies using the *ok107-Gal4* driver has no effect on either spatial or temporal parameters in Buridan's paradigm.

There are two reasons for knocking out *FoxP* in motorneurons, besides *FoxP* expression there (Fig. 3): first, networks of motorneurons in the VNC control movement patterns and walking is directly affected by our manipulations so far (Figs. 6, 7). Second, motorneurons were shown to be important for the type of operant self-learning that also requires *FoxP* (Colomb and Brembs, 2016). Driving expression of gRNA/Cas9 with either of two motorneuron-specific driver lines (*D42-Gal4* and *C380-Gal4*) led to a significant alteration in locomotor activity in Buridan's paradigm, both for spatial and for temporal parameters. (Fig. 10A, B; raw data deposited at 10.6084/m9.figshare.12607823).

Perhaps the most prevalent *FoxP* expression can be observed in the protocerebral bridge (PB, Fig. 1). The driver line *cmpy-Gal4* targets the PB specifically and drives expression in *FoxP*-positive neurons (Fig. 10C). Removing the *FoxP* gene exclusively in these neurons led to a significant reduction of locomotor activity (Fig. 10D) as well as a reduction in stripe fixation and to more tortuous trajectories (Fig. 10E).

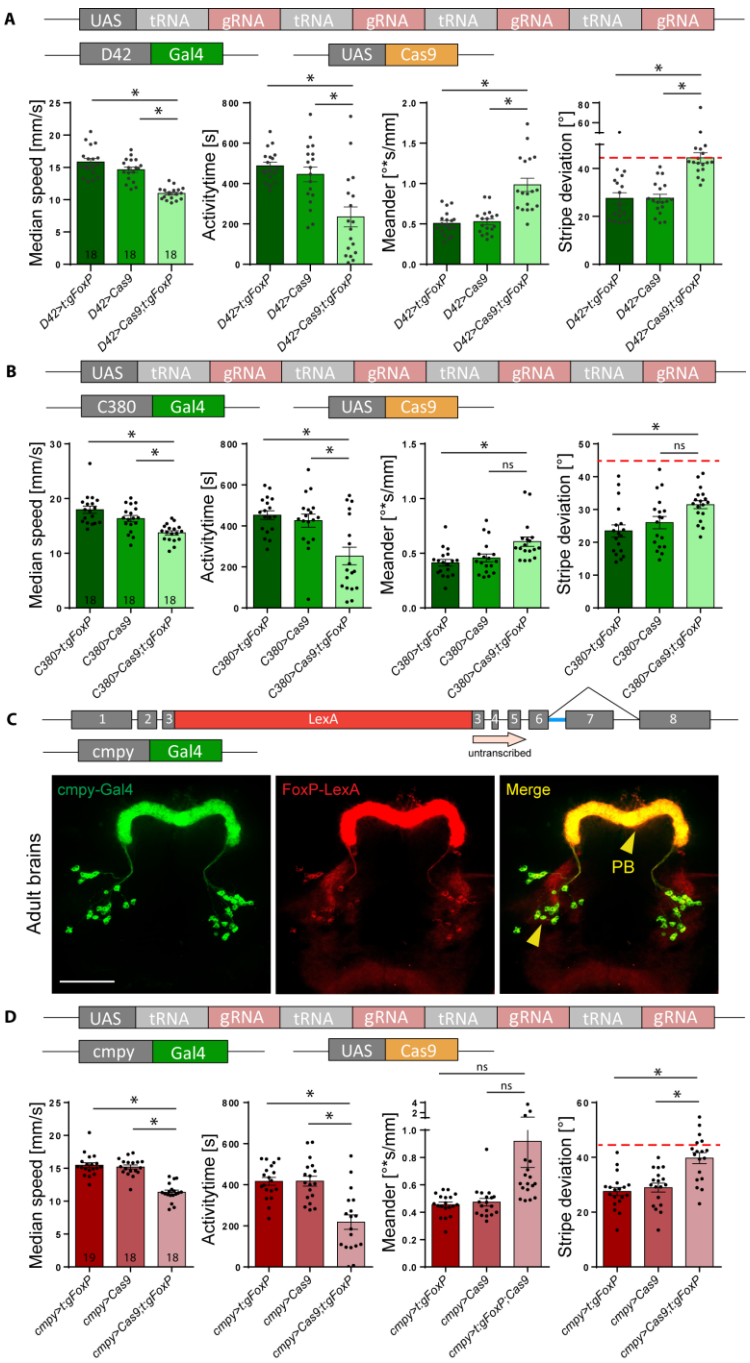

Fig. 10: FoxP *is required in both motorneurons and protocerebral bridge for normal walking behavior in Buridan's paradigm.*
(A, B) Both motorneuron-specific driver lines *D42-Gal4* (A) and *C380-Gal4* (B) show similar reductions in walking speed and activity time, combined with an increase in stripe deviation, indicating poorer stripe fixation. The reduction in activity time for *D42* fails to reach statistical significance, apparently due to a low value for the Cas9 control line. (C) The *cmpy-Gal4* driver stains an overlapping set of protocerebral bridge (PCB) neurons compared to our *FoxP-LexA* driver line. (D) Knocking out the *FoxP* gene in *cmpy-Gal4*-positive neurons leads to similar alterations in walking behavior in Buridan's paradigm as a complete knock-out, i.e., reduced walking speed, reduced activity time, decreased stripe fixation and increased meander. *p<0.005.

3.8. Conditional *FoxP-KO*: developmental stages

With *FoxP* being a transcription factor active throughout development and particularly important during pupal development (Castells-Nobau et al., 2019; Schatton and Scharff, 2017), we knocked out *FoxP* in all neurons by adding the Gal4 repressor Gal80^{ts} to our pan-neuronal *FoxP-cKO* (Fig. 11A; raw data deposited at 10.6084/m9.figshare.12607838) and treating the flies with a 48 hrs 30 °C heat treatment during the early pupal stage. This regime did not affect walking behavior in Buridan's paradigm (Fig. 11B). Shifting the temperature treatment to immediately after eclosion also did not affect the flies' behavior in Buridan's paradigm (Fig. 11C). Taken together, these data indicate that *FoxP* is required for the proper development of, for instance, motor neurons and PB neurons, but once these circuitries are in place, FoxP expression does not appear to have any immediate mechanistic role in locomotion any more.

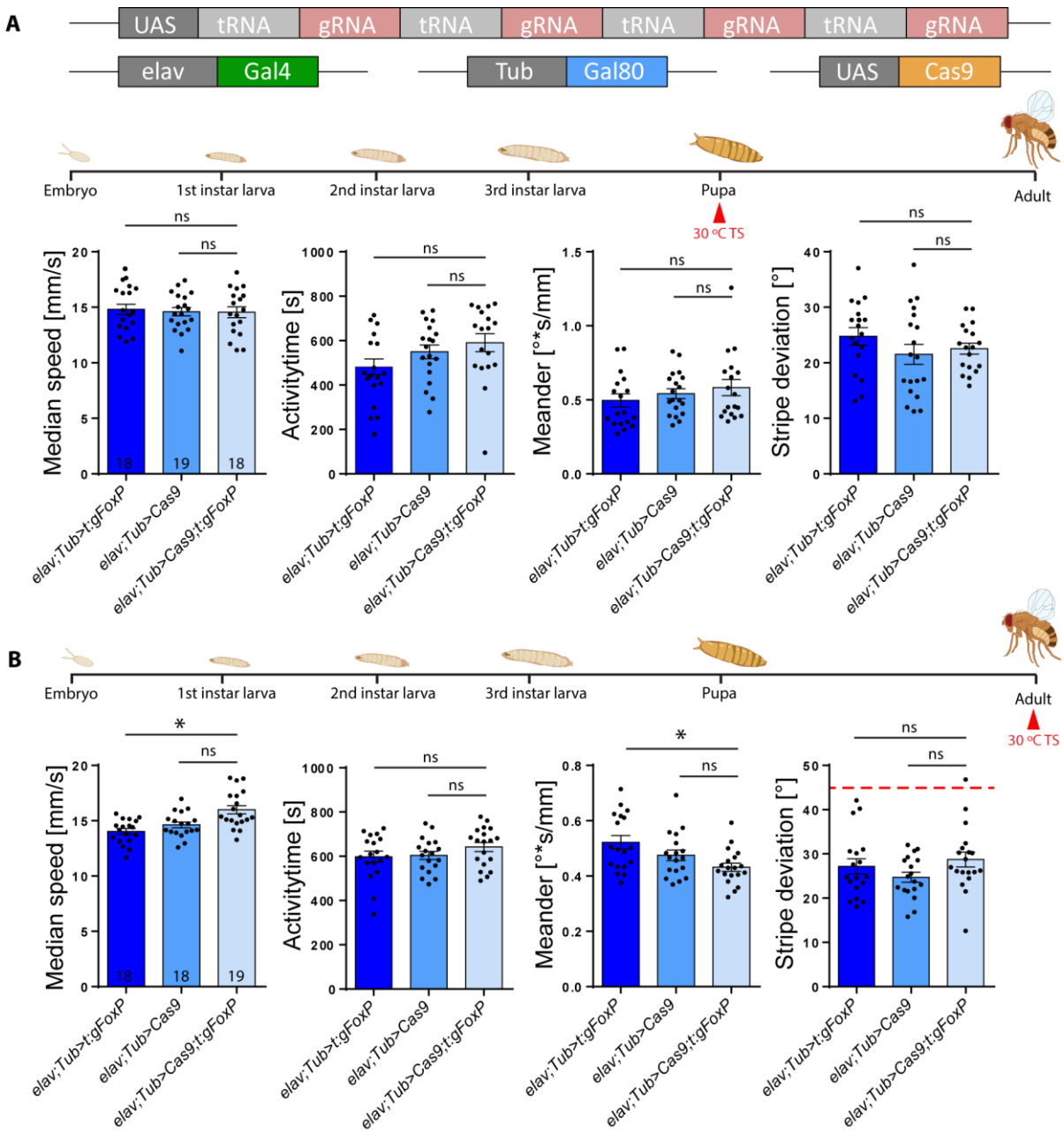

Fig. 11: *Adult* FoxP *expression is not required for normal locomotor behavior in Buridan's paradigm*. (A) Genetic tools used to perform the temporally controlled FoxP knock out. (B) Neither temporal (median speed and activity time) nor spatial (meander and stripe deviation) parameters are altered in adult flies in Buridan's paradigm after inducing the FoxP KO in the early pupa. (C) Neither temporal nor spatial parameters are changed in adult flies in Buridan's paradigm after inducing the FoxP KO immediately after eclosion. *p<0.005.

4. Discussion

We have edited the genomic locus of the *Drosophila FoxP* gene in order to better understand the expression patterns of the *FoxP* isoforms and their involvement in behavior. We have discovered that the isoforms differ with respect to their expression in neuronal tissue. For instance, we found isoform B (*FoxP-iB*) expression in neuropil areas such as the superior medial protocerebrum, the protocerebral bridge, the noduli, the vest, the saddle, the gnathal ganglia and the medulla, while areas such as the antennal lobes, the fan shaped body, the lobula and a glomerulus of the posterior ventrolateral protocerebrum contain other *FoxP* isoforms but not isoform B (summarized in Fig. 12) (raw data deposited at 10.6084/m9.figshare.12607862). We also corroborated previous results (Castells-Nobau et al., 2019) that *FoxP* is expressed in a large variety of neuronal cell types (Fig. 3). Our genomic manipulations created several new alleles of the *FoxP* gene which had a number of behavioral consequences that mimicked other, previously published alleles (Castells-Nobau et al., 2019). Specifically, we found that constitutive knockout of either *FoxP-IB* alone or of all *FoxP* isoforms affects several parameters of locomotor behavior, such as walking speed,

the straightness of walking trajectories or landmark fixation (Figs. 6, 7). We discovered that mutating the *FoxP* gene only in particular neurons can have different effects. For instance, knocking *FoxP* out in neurons of the dorsal cluster (where *FoxP* is expressed) or in mushroom body Kenyon cells (where neither we nor (Castells-Nobau et al., 2019) were able to detect FoxP expression) had no effect in Buridan's paradigm (Fig. 9), despite these neurons being required for normal locomotion in Buridan's paradigm (Linneweber et al., 2020; Serway et al., 2009; Xiong et al., 2010). In contrast, without *FoxP* in the protocerebral bridge or motor neurons, flies show similar locomotor impairments as flies with constitutive knockouts (Fig. 10). These impairments appear to be due to developmental action of the *FoxP* gene during larval development, as no such effects can be found if the gene is knocked out in all cells in the early pupal or adult stages (Fig. 11).

4.1. *FoxP* expression

4.1.1. Neuronal expression of *FoxP* is widespread but not in mushroom bodies

The exact expression pattern of *FoxP* has been under debate for quite some time now. Initial work combined traditional reporter gene expression with immunohistochemistry (Lawton et al., 2014). Lawton and colleagues (2014) created a *FoxP-Gal4* line where a 1.5 kb

1076 fragment of genomic DNA upstream of the
1077 *FoxP* coding region was used as a promoter to
1078 drive Gal4 expression. These authors
1079 compared the resulting expression pattern
1080 with the staining of a commercial polyclonal
1081 antibody against FoxP. This was the same
1082 antibody which we have used in this study and
1083 which we validated as faithfully reporting FoxP
1084 expression patterns (Fig. 1C). Their description
1085 of the *FoxP* expression pattern as a small
1086 number of neurons distributed in various
1087 areas of the brain, particularly in the
1088 protocerebral bridge (PCB), matches our
1089 results and those of (Castells-Nobau et al.,
1090 2019).

1091 Also in the second and third published
1092 reports on *FoxP* expression patterns in
1093 *Drosophila* (DasGupta et al., 2014; Schatton
1094 and Scharff, 2017), the authors used putative
1095 *FoxP* promoter fragments to direct the
1096 expression of Gal4. The earlier publication
1097 used a 1.4kb sequence upstream of the *FoxP*
1098 transcription start site, while the later took 1.9
1099 kb. Their larger fragment contained the
1100 sequences of the two previously used
1101 fragments. In contrast to (Castells-Nobau et al.,
1102 2019; Lawton et al., 2014) and our work here,
1103 both studies reported expression in
1104 overlapping sets of mushroom body Kenyon
1105 cells. While the earlier work implied that there
1106 was no expression outside of the mushroom

bodies, the later was not explicit. However, Schatton *et al.* independently reported that they had observed strong expression also outside of the mushroom bodies ((Schatton, 2018) and pers. comm.).

The fourth study reporting on *FoxP* expression in *Drosophila (Castells-Nobau et al., 2019)* avoided the promoter fragment method but tagged *FoxP* within a genomic segment contained in a fosmid (Kim et al., 1992), intended to ensure expression of GFP-tagged *FoxP* under the control of its own, endogenous regulatory elements. This study was the first to circumvent the potential for artifacts created either by selection of the wrong promoter fragment or by choosing an inappropriate basal promoter with the fragment. However, since they also used insertion of a transgene, their expression pattern, analogous to that of a promoter fragment Gal4 line, may potentially be subject to local effects where the fosmid with the tagged *FoxP* was inserted. Castells-Nobau and colleagues (2019) also used the antibody generated by Lawton et al. (2014) to validate their transgenic expression patterns. The results reported with this technique are similar to those of Lawton et al. (2014) and our work (summarized in Fig. 12B).

In an attempt to eliminate the last source of error for determining the expression pattern of FoxP in *Drosophila*, we used

CRISPR/Cas9 with homology-directed repair to tag *FoxP in situ*, avoiding both the potential local insertion effects of the previous approaches and without disrupting the complex regulation that may occur from more distant parts in the genome. For instance, in human cells, there are at least 18 different genomic regions that are in physical contact with the *FOXP2* promoter, some of which act as enhancers (Becker et al., 2018). The effects of these regions may be disrupted even if the entire genomic *FoxP* locus were inserted in a different genomic region as in (Castells-Nobau et al., 2019). Interestingly, the first promoter fragment approach (Lawton et al., 2014) and the fosmid approach (Castells-Nobau et al., 2019) agree both with our most artifact-avoiding genome editing approach and the immunohistochemistry with an antibody validated by at least three different *FoxP-KO* approaches. This converging evidence from four different methods used in three different laboratories suggests that *FoxP* is expressed in about 1800 neurons in the fly nervous system, of which about 500 are located in the ventral nerve cord. Expression in the brain is widespread with both localized clusters and individual neurons (Fig. 12B) across a variety of neuronal cell types. Notably, the four methods also agree that there is no detectable *FoxP* expression in the adult or larval mushroom

bodies. In contrast, in honey bees, there is converging evidence of FoxP expression in the MBs (Schatton and Scharff, 2017).

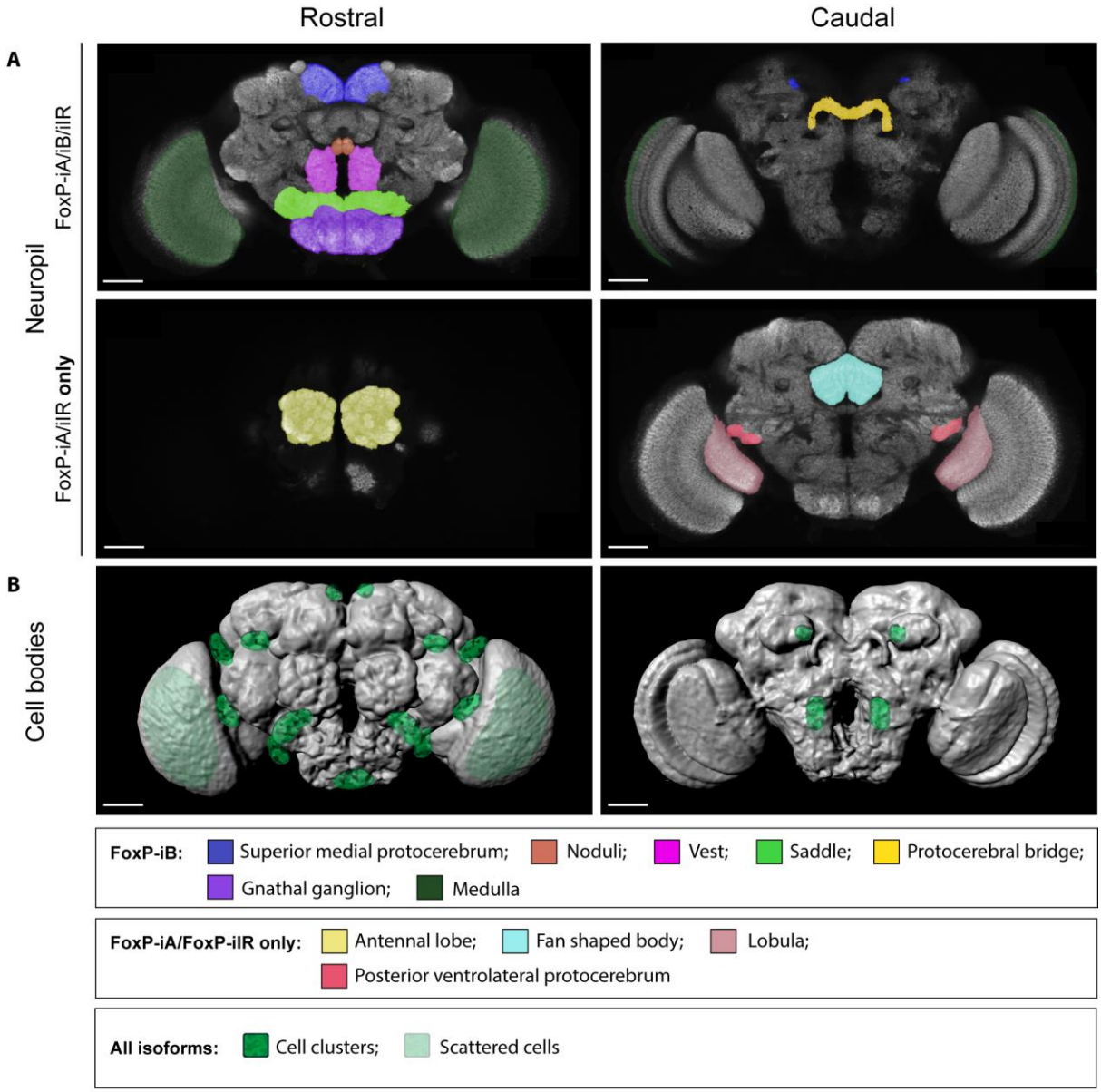

Fig. 12: FoxP *expression pattern in the adult* Drosophila *brain*.
(A) Rostral and caudal sections with neuropil areas marked for *FoxP-iB* expression (above) or for other *FoxP* isoforms excluding *FoxP-iB* (below). (B) Volume rendering of adult neuropil with marked approximate *FoxP*-positive cell body locations in the cortex. Scale bars: 50 µm.

4.1.2. Different *FoxP* isoforms are expressed in different neurons

Our genome editing approach allowed us to distinguish differences in the expression patterns of different FoxP isoforms. The isoform specifically involved in operant self-learning, *FoxP-iB*, is only expressed in about 65% of all *FoxP*-positive neurons. The remainder express either *FoxP-iA* or *FoxP-iIR* or both. These neurons are localized in the antennal lobes, the fan-shaped body, the lobula and a glomerulus of the posterior ventrolateral protocerebrum. Combined with all three isoforms differing in their DNA-binding FH box, the different expression patterns for the different isoforms adds to the emerging picture that the different isoforms may serve very different functions.

4.2. *FoxP* and locomotor behavior

4.2.1. *FoxP* is involved in both spatial and temporal parameters of walking

Alterations of *FoxP* family genes universally result in various motor deficits on a broad scale in humans (Carr et al., 2010; den Hoed and Fisher, 2020; Palumbo et al., 2013; Reuter et al., 2017) and mice (Chabout et al., 2016; French et al., 2019; Usui et al., 2017) for both learned and innate behaviors. Also in flies, manipulations of the *FoxP* locus by mutation or RNA interference have revealed that *FoxP* is involved in flight performance and

other, presumably inborn, locomotor behaviors (Castells-Nobau et al., 2019; Kottler et al., 2019; Lawton et al., 2014; Mendoza et al., 2014) as well as in motor learning tasks (Mendoza et al., 2014).

The locomotor phenotypes described so far largely concerned the temporal aspects of locomotion, such as initiation, speed or duration of locomotor behaviors. Here, using Buridan's paradigm (Colomb et al., 2012; Götz, 1980), we report that manipulations of *FoxP* can also alter spatial aspects of locomotion, such as landmark fixation or the straightness of trajectories. Our results further exemplify the old insight that coarse assaults on gene function such as constitutive knock-outs of entire genes or isoforms very rarely yield useful, specific phenotypes (Pflugfelder, 1998). Rather, it is often the most delicate of manipulations that reveal the involvement of a particular gene in a specific behavior. This fact is likely most often due to the pleiotropy of genes, often paired with differential dominance which renders coarse neurogenetic approaches useless in most instances, as so many different behaviors are affected that the specific contribution of a gene to a behavioral phenotype becomes impossible to dissect.

In the case of *FoxP*, it was already known, for instance, that the different isoforms affect

flight performance to differing degrees (Mendoza et al., 2014) and that a variety of different *FoxP* manipulations affected general locomotor activity (Castells-Nobau et al., 2019; Kottler et al., 2019; Lawton et al., 2014). Here we show that a complete knock-out of either *FoxP-iB* or all isoforms affected both spatial and temporal parameters of locomotion, but the insertion mutation $FoxP^{3955}$ altered only temporal parameters (Figs. 6, 7). Interestingly, despite the ubiquitous and substantial locomotor impairments after nearly any kind of *FoxP* manipulation be it genomic or via RNAi reported in the published literature, DasGupta et al. (2014), failed to detect these locomotor defects of these flies.

While some of our manipulations did not affect locomotion at all (e.g. knock-out in MBs or DCNs, Fig. 9, see below for discussion), most of them affected both spatial and temporal locomotion parameters (e.g., Figs. 6, 7, 9), despite these parameters commonly not co-varying (Colomb and Brembs, 2014). Thus, while one would expect these behaviors to be biologically separable, our manipulations did not succeed in this separation. The only case where only one set of parameters was affected were the $FoxP^{3955}$ mutant flies (Fig. 6). However, the genetic background used in these experiments (Canton S from the laboratory of the late Troy Zars) already shows strikingly

weak landmark fixation (Colomb and Brembs, 2014). It is thus not entirely clear if this separation is due to the mutant allele or the genetic background or some interaction of the two. Until further results have been obtained, the conspicuous fact remains that statistically non-covarying traits do not seem to readily segregate with *FoxP* manipulations.

4.2.2. Locomotion does not require FoxP expression in all *FoxP* neurons

Taken together, the results available todate reveal *FoxP* to be a highly pleiotropic gene with phenotypes that span both temporal and spatial domains of locomotion in several behavioral modalities, lifespan, motor learning, social behavior and habituation. It is straightforward to conclude that only precise, cell-type specific *FoxP* manipulations of specific isoforms will be capable of elucidating the function this gene serves in each phenotype. With RNAi generally yielding varying levels of knock-down and, specifically, with currently available *FoxP* RNAi lines showing only little, if any, detectable knock-down with RT-qPCR (data deposited at 10.6084/m9.figshare.12607667 and Annette Schenck, pers. comm.), CRISPR/Cas9-mediated genome editing lends itself as the method of choice for this task. Practical considerations when designing multi-target gRNAs for *FoxP* prompted us to begin testing the CRISPR/Cas9

system as an alternative to RNAi with an isoform-unspecific approach first, keeping the isoform-specific approach for a time when we have collected more experience in this technique. In a first proof-of-principle, we used CRISPR/Cas9 to remove *FoxP* from mushroom-body Kenyon cells (MBs), dorsal cluster neurons (DCNs), motor neurons (MNs) and the protocerebral bridge (PCB).

MBs have been shown to affect both spatial and temporal aspects of locomotion (Besson and Martin, 2005; Helfrich-Förster et al., 2002; Lark et al., 2017; Lebreton and Martin, 2009; Mabuchi et al., 2016; Manjila et al., 2019; e.g., Martin et al., 1998; Serway et al., 2009; Sun et al., 2018; Xiong et al., 2010) and Castells-Nobau et al. (Castells-Nobau et al., 2019) reported a subtle structural phenotype in a subset of MB Kenyon cells that did not express *FoxP*. Moreover, DasGupta et al. (2014) as well as Groschner et al. (2018) used two different methods to show that *FoxP* is expressed in MBs, while neither we nor (Lawton et al., 2014) nor (Castells-Nobau et al., 2019) were able to detect *FoxP* in MBs. With a substantial walking defect both in $FoxP^{3955}$ mutant flies (which primarily affects *FoxP-iB* expression (Mendoza et al., 2014)) and in flies without any *FoxP* (Fig. 7), together with the MBs being critical for normal walking behavior, the MBs were a straightforward candidate for a cell-type-

specific *FoxP-KO*. However, flies without *FoxP* in the MBs walk perfectly normally (Fig. 9C). There are two possible reasons for this lack of an effect of our manipulation: either *FoxP* is not expressed in MBs or it is not important in MBs for walking. While at this point we are not able to decide between these two options, our expression data concurring with those from previous studies (Castells-Nobau et al., 2019; Lawton et al., 2014) suggest the former explanation may be the more likely one. Interestingly, a publication that did report *FoxP* expression in the MBs (DasGupta et al., 2014) did not detect the walking deficits in $FoxP^{3955}$ mutant flies despite testing for such effects. Motor aberrations as those described here and in other *FoxP* manipulations (Castells-Nobau et al., 2019; Kottler et al., 2019; Lawton, 2014; Lawton et al., 2014) constitute a potential alternative to the decision-making impairments ascribed to these flies in DasGupta *et al*..

DCNs were recently shown to be involved in the spatial component (landmark fixation) of walking in Buridan's paradigm (Linneweber et al., 2020), but removing *FoxP* from DCNs showed no effect (Fig. 9B), despite abundant *FoxP* expression in DCNs (Fig. 9A). In this case, the only explanation is that *FoxP* is not required in these neurons for landmark

fixation in Buridan's paradigm, while the neurons themselves are required.

MNs are involved in all aspects of behavior and have been shown to be important for operant self-learning (Colomb and Brembs, 2016). With abundant expression of *FoxP* in MNs (Fig. 3A), we considered these neurons a prime candidate for a clear *FoxP-cKO* phenotype. Indeed, removing FoxP specifically from MNs only, mimicked the effects of removing the gene constitutively from all cells (Fig. 10A, B). It is noteworthy that this manipulation alone was sufficient to affect both temporal and spatial parameters, albeit only one of the two driver lines showed clear-cut results (D42). One would not necessarily expect motorneurons to affect purportedly 'higher-order' functions such as landmark fixation. It is possible that the higher tortuosity in the trajectories of the flies where D42 was used to drive our UAS-gRNA construct is largely responsible for the greater angular deviation from the landmarks in these flies and that this tortuosity, in turn is caused by the missing FoxP in motorneurons. Alternatively, D42 is also driving in non-motorneurons where *FoxP* is responsible for landmark fixation. The driver line C380 showed similar trends, albeit not quite statistically significant at our alpha value of 0.5%, suggesting that potentially the

increased meander parameter may be caused by motorneurons lacking *FoxP*.

The PB is not only the arguably most conspicuous *FoxP*-positive neuropil, it has also been reported to be involved in temporal aspects of walking (Martin et al., 1999; Poeck et al., 2008; Strauss et al., 1992). Moreover, the PB provides input to other components of the central complex involved in angular orientation (Kim et al., 2019; Kottler et al., 2019; Seelig and Jayaraman, 2015; Su et al., 2017). Similar to the results in MNs, removing *FoxP* from a small group of brain neurons innervating the PB, phenocopies constitutive *FoxP* mutants.

Taken together, the MN and PB results suggest that both sets of neurons serve their locomotor function in sequence. At this point, it is unclear which set of neurons should precede the other in this sequence. In this example of locomotion, it is straightforward to hypothesize that central neurons would be active before the MNs coordinate the movements. However, in, e.g., operant self-learning, MNs may contribute to the necessary behavioral variability underlying the learning process, such that central neurons could be active after the MNs (in the hypothetical case that also in learning both neuronal populations were found to be required in sequence (work in progress)).

4.2.3. *FoxP* is only required during larval development to ensure normal locomotion

There is ample evidence that the *FoxP* family of transcription factors acts during development in a variety of tissues (Co et al., 2020; Lu et al., 2002; Shu et al., 2007). What is less well known is if adult *FoxP* expression serves any specific function. A recent study in transgenic mice in operant conditioning and motor learning tasks showed postnatal knock-out of FOXP2 in cerebellar and striatal neurons affected leverpressing and cerebellar knock-out also affected motor-learning (French et al., 2019). At least for these tasks in mammals, a *FoxP* family member does serve a postnatal function that is independent of brain development (brain morphology was unaltered in these experiments). Also in birds, evidence has been accumulating that adult *FoxP* expression serves a song plasticity function (Chen et al., 2013; Day et al., 2019; Miller et al., 2008; Shi et al., 2013; Teramitsu and White, 2006; Thompson et al., 2013). Our temporally controlled experiments (Figs. 8, 11) suggest that at least locomotion in Buridan's paradigm can function normally in the absence of *FoxP* expression in the adult, as long as *FoxP* expression remains unaltered during larval development. Future experiments will test other phenotypes for adult *FoxP* requirement.

Acknowledgements

Technical assistance was provided by Klara Krmpotić (Buridan experiments with *FoxP-iB-Gal4*) and Anders Eriksson (statistical analysis and fly drawings). We are indebted to David Deitcher for sharing his FoxP antibody with us. This project was funded by the DFG (Deutsche Forschungsgemeinschaft, grant BR 1892/17-1). All original raw data are deposited with figshare (http://figshare.com), references in the text.

Author contributions

Conceived and designed the experiments: OP, MR, BB. Performed the experiments: OP. Analyzed the data: OP, MR, BB. Contributed reagents/materials/analysis tools: MR, BB. Wrote the paper: OP, BB. Initiated the project: BB. Critically revised the manuscript: OP, MR, BB. The authors declare no existing conflicts of interest.

References

Becker M, Devanna P, Fisher SE, Vernes SC. 2018. Mapping of Human FOXP2 Enhancers Reveals Complex Regulation. *Front Mol Neurosci* **11**:47.

Benjamin DJ, Berger JO, Johannesson M, Nosek BA, Wagenmakers E-J, Berk R, Bollen KA, Brembs B, Brown L, Camerer C, Cesarini D, Chambers CD, Clyde M, Cook TD, De Boeck P, Dienes Z, Dreber A, Easwaran K, Efferson C, Fehr E, Fidler F, Field AP, Forster M, George EI, Gonzalez R, Goodman S, Green E, Green DP, Greenwald AG, Hadfield JD, Hedges LV, Held L, Hua Ho T, Hoijtink H, Hruschka DJ, Imai K, Imbens G, Ioannidis JPA, Jeon M, Jones JH, Kirchler M, Laibson D, List J, Little R, Lupia A, Machery E, Maxwell SE, McCarthy M, Moore DA, Morgan SL, Munafó M, Nakagawa S, Nyhan B, Parker TH, Pericchi L, Perugini M, Rouder J, Rousseau J, Savalei V, Schönbrodt FD, Sellke T, Sinclair B, Tingley D, Van Zandt T, Vazire S, Watts DJ, Winship C, Wolpert RL, Xie Y, Young C, Zinman J, Johnson VE. 2018. Redefine statistical significance. *Nat Hum Behav* **2**:6–10.

Besson M, Martin J-R. 2005. Centrophobism/thigmotaxis, a new role for the mushroom bodies in Drosophila. *J Neurobiol* **62**:386–396.

Bolhuis JJ. 2011. Twitter evolution: Parallel brain mechanisms of auditory–vocal learning in songbirds and humans. *Neuroscience Research*. doi:10.1016/j.neures.2011.07.080

Carr CW, Moreno-De-Luca D, Parker C, Zimmerman HH, Ledbetter N, Martin CL, Dobyns WB, Abdul-Rahman OA. 2010. Chiari I malformation, delayed gross motor skills, severe speech delay, and epileptiform discharges in a child with FOXP1 haploinsufficiency. *Eur J Hum Genet* **18**:1216–1220.

Castells-Nobau A, Eidhof I, Fenckova M, Brenman-Suttner DB, Scheffer-de Gooyert JM, Christine S,

Schellevis RL, van der Laan K, Quentin C, van Ninhuijs L, Hofmann F, Ejsmont R, Fisher SE, Kramer JM, Sigrist SJ, Simon AF, Schenck A. 2019. Conserved regulation of neurodevelopmental processes and behavior by FoxP in Drosophila. *PLoS One* **14**:e0211652.

Chabout J, Sarkar A, Patel SR, Radden T, Dunson DB, Fisher SE, Jarvis ED. 2016. A Foxp2 Mutation Implicated in Human Speech Deficits Alters Sequencing of Ultrasonic Vocalizations in Adult Male Mice. *Front Behav Neurosci* **10**:197.

Chen Q, Heston JB, Burkett ZD, White SA. 2013. Expression analysis of the speech-related genes FoxP1 and FoxP2 and their relation to singing behavior in two songbird species. *J Exp Biol* **216**:3682–3692.

Colomb J, Brembs B. 2016. PKC in motorneurons underlies self-learning, a form of motor learning in Drosophila. *PeerJ* **4**:e1971.

Colomb J, Brembs B. 2014. Sub-strains of Drosophila Canton-S differ markedly in their locomotor behavior. *F1000Research*. doi:10.12688/f1000research.4263.1

Colomb J, Reiter L, Blaszkiewicz J, Wessnitzer J, Brembs B. 2012. Open source tracking and analysis of adult Drosophila locomotion in Buridan's paradigm with and without visual targets. *PLoS One* **7**:e42247.

Co M, Anderson AG, Konopka G. 2020. FOXP transcription factors in vertebrate brain development, function, and disorders. *Wiley Interdiscip Rev Dev Biol* e375.

DasGupta S, Ferreira CH, Miesenböck G. 2014. FoxP influences the speed and accuracy of a perceptual decision in Drosophila. *Science* **344**:901–904.

Day NF, Hobbs TG, Heston JB, White SA. 2019. Beyond Critical Period Learning: Striatal FoxP2 Affects the Active Maintenance of Learned Vocalizations in Adulthood. *eNeuro* **6**. doi:10.1523/ENEURO.0071-19.2019

den Hoed J, Fisher SE. 2020. Genetic pathways involved in human speech disorders. *Curr Opin Genet Dev* **65**:103–111.

Diao F, Ironfield H, Luan H, Diao F, Shropshire WC, Ewer J, Marr E, Potter CJ, Landgraf M, White BH. 2015. Plug-and-play genetic access to drosophila cell types using exchangeable exon cassettes. *Cell Rep* **10**:1410–1421.

Dolan M-J, Belliart-Guérin G, Bates AS, Frechter S, Lampin-Saint-Amaux A, Aso Y, Roberts RJV, Schlegel P, Wong A, Hammad A, Bock D, Rubin GM, Preat T, Plaçais P-Y, Jefferis GSXE. 2018. Communication from Learned to Innate Olfactory Processing Centers Is Required for Memory Retrieval in Drosophila. *Neuron* **100**:651–668.e8.

Fee MS. 2014. The role of efference copy in striatal learning. *Curr Opin Neurobiol* **25**:194–200.

Felsenberg J, Jacob PF, Walker T, Barnstedt O, Edmondson-Stait AJ, Pleijzier MW, Otto N, Schlegel P, Sharifi N, Perisse E, Smith CS, Lauritzen JS, Costa M, Jefferis GSXE, Bock DD, Waddell S. 2018. Integration of Parallel Opposing Memories Underlies Memory Extinction. *Cell* **175**:709–722.e15.

French CA, Vinueza Veloz MF, Zhou K, Peter S, Fisher SE, Costa RM, De Zeeuw CI. 2019. Differential effects of Foxp2 disruption in distinct motor circuits. *Mol Psychiatry* **24**:447–462.

Golson ML, Kaestner KH. 2016. Fox transcription factors: from development to disease. *Development* **143**:4558–4570.

Götz KG. 1980. Visual guidance in Drosophila. *Basic Life Sci* **16**:391–407.

Groschner LN, Chan Wah Hak L, Bogacz R, DasGupta S, Miesenböck G. 2018. Dendritic Integration of Sensory Evidence in Perceptual Decision-Making. *Cell* **173**:894–905.e13.

Haesler S, Rochefort C, Georgi B, Licznerski P, Osten P, Scharff C. 2007. Incomplete and inaccurate vocal imitation after knockdown of FoxP2 in songbird basal ganglia nucleus Area X. *PLoS Biol* **5**:e321.

Hagoort P. 2019. Human Language: From Genes and Brains to Behavior. MIT Press.

Hannenhalli S, Kaestner KH. 2009. The evolution of Fox genes and their role in development and disease. *Nat Rev Genet* **10**:233–240.

Hassan BA, Bermingham NA, He Y, Sun Y, Jan YN, Zoghbi HY, Bellen HJ. 2000. atonal regulates neurite arborization but does not act as a proneural gene in the Drosophila brain. *Neuron* **25**:549–561.

Helfrich-Förster C, Wulf J, de Belle JS. 2002. Mushroom body influence on locomotor activity and circadian rhythms in Drosophila melanogaster. *J Neurogenet* **16**:73–109.

Horn D, Kapeller J, Rivera-Brugués N, Moog U, Lorenz-Depiereux B, Eck S, Hempel M, Wagenstaller J, Gawthrope A, Monaco AP, Bonin M, Riess O, Wohlleber E, Illig T, Bezzina CR, Franke A, Spranger S, Villavicencio-Lorini P, Seifert W, Rosenfeld J, Klopocki E, Rappold GA, Strom TM. 2010. Identification of FOXP1 deletions in three unrelated patients with mental retardation and significant speech and language deficits. *Hum Mutat* **31**:E1851–60.

Kim SS, Hermundstad AM, Romani S, Abbott LF, Jayaraman V. 2019. Generation of stable heading representations in diverse visual scenes. *Nature* **576**:126–131.

Kim UJ, Shizuya H, de Jong PJ, Birren B, Simon MI. 1992. Stable propagation of cosmid sized human DNA inserts in an F factor based vector. *Nucleic Acids Res* **20**:1083–1085.

König C, Khalili A, Niewalda T, Gao S, Gerber B. 2019. An optogenetic analogue of second-order reinforcement in Drosophila. *Biol Lett* **15**:20190084.

Kottler B, Faville R, Bridi JC, Hirth F. 2019. Inverse Control of Turning Behavior by Dopamine D1 Receptor Signaling in Columnar and Ring Neurons of the Central Complex in Drosophila. *Curr Biol* **29**:567–577.e6.

Lai CS, Fisher SE, Hurst JA, Vargha-Khadem F, Monaco AP. 2001. A forkhead-domain gene is mutated in a severe speech and language disorder. *Nature* **413**:519–523.

Lark A, Kitamoto T, Martin J-R. 2017. Modulation of neuronal activity in the Drosophila mushroom body by DopEcR, a unique dual receptor for ecdysone and dopamine. *Biochim Biophys Acta Mol Cell Res* **1864**:1578–1588.

Lawton K. 2014. Conserved Role Of Drosophila Melanogaster Foxp In Motor Coordination And Courtship Song (PhD). Cornell University.

Lawton KJ, Wassmer TL, Deitcher DL. 2014. Conserved role of Drosophila melanogaster FoxP in motor coordination and courtship song. *Behav Brain Res* **268**:213–221.

Lebreton S, Martin J-R. 2009. Mutations affecting the cAMP transduction pathway disrupt the centrophobism behavior. *J Neurogenet* **23**:225–234.

Linneweber GA, Andriatsilavo M, Dutta SB, Bengochea M, Hellbruegge L, Liu G, Ejsmont RK, Straw AD, Wernet M, Hiesinger PR, Hassan BA. 2020. A neurodevelopmental origin of behavioral individuality in the Drosophila visual system. *Science* **367**:1112–1119.

Lu MM, Li S, Yang H, Morrisey EE. 2002. Foxp4: a novel member of the Foxp subfamily of winged-helix genes co-expressed with Foxp1 and Foxp2 in pulmonary and gut tissues. *Mech Dev* **119 Suppl 1**:S197–202.

Lyutova R, Selcho M, Pfeuffer M, Segebarth D, Habenstein J, Rohwedder A, Frantzmann F, Wegener C, Thum AS, Pauls D. 2019. Reward signaling in a recurrent circuit of dopaminergic neurons and peptidergic Kenyon cells. *Nat Commun* **10**:3097.

Mabuchi I, Shimada N, Sato S, Ienaga K, Inami S, Sakai T. 2016. Mushroom body signaling is required for locomotor activity rhythms in Drosophila. *Neurosci Res* **111**:25–33.

Manjila SB, Kuruvilla M, Ferveur J-F, Sane SP, Hasan G. 2019. Extended Flight Bouts Require Disinhibition from GABAergic Mushroom Body Neurons. *Curr Biol* **29**:283–293.e5.

Marler P. 1991. Song-learning behavior: The interface with neuroethology. *Trends Neurosci* **14**:199–206.

Martin JR, Ernst R, Heisenberg M. 1998. Mushroom bodies suppress locomotor activity in Drosophila melanogaster. *Learn Mem* **5**:179–191.

Martin JR, Raabe T, Heisenberg M. 1999. Central complex substructures are required for the maintenance of locomotor activity in Drosophila melanogaster. *J Comp Physiol A* **185**:277–288.

McGuire SE, Le PT, Osborn AJ, Matsumoto K, Davis RL. 2003. Spatiotemporal rescue of memory dysfunction in Drosophila. *Science* **302**:1765–1768.

McGuire SE, Mao Z, Davis RL. 2004. Spatiotemporal gene expression targeting with the TARGET and gene-switch systems in Drosophila. *Sci STKE* **2004**:l6.

Mendoza E, Colomb J, Rybak J, Pflüger H-J, Zars T, Scharff C, Brembs B. 2014. Drosophila FoxP mutants are deficient in operant self-learning. *PLoS One* **9**:e100648.

Miller JE, Spiteri E, Condro MC, Dosumu-Johnson RT, Geschwind DH, White SA. 2008. Birdsong decreases protein levels of FoxP2, a molecule required for human speech. *J Neurophysiol* **100**:2015–2025.

Morgan A, Fisher SE, Scheffer I, Hildebrand M. 2016. Related Speech and Language Disorders In: Adam MP, Ardinger HH, Pagon RA, Wallace SE, Bean LJH, Stephens K, Amemiya A, editors. GeneReviews. Seattle (WA): University of Washington, Seattle.

Naour P. 2009. E.O. Wilson and B.F. Skinner. New York, NY: Springer New York.

Palumbo O, D'Agruma L, Minenna AF, Palumbo P, Stallone R, Palladino T, Zelante L, Carella M. 2013. 3p14.1 de novo microdeletion involving the FOXP1 gene in an adult patient with autism, severe speech delay and deficit of motor coordination. *Gene* **516**:107–113.

Pflugfelder GO. 1998. Genetic lesions in Drosophila behavioural mutants. *Behav Brain Res* **95**:3–15.

Poeck B, Triphan T, Neuser K, Strauss R. 2008. Locomotor control by the central complex in Drosophila-An analysis of the tay bridge mutant. *Dev Neurobiol* **68**:1046–1058.

Pollock JA, Ellisman MH, Benzer S. 1990. Subcellular localization of transcripts in Drosophila photoreceptor neurons: chaoptic mutants have an aberrant distribution. *Genes Dev* **4**:806–821.

Port F, Bullock SL. 2016. Augmenting CRISPR applications in Drosophila with tRNA-flanked sgRNAs. *Nat Methods* **13**:852–854.

Reuter MS, Riess A, Moog U, Briggs TA, Chandler KE, Rauch A, Stampfer M, Steindl K, Gläser D, Joset P, DDD Study, Krumbiegel M, Rabe H, Schulte-Mattler U, Bauer P, Beck-Wödl S, Kohlhase J, Reis A, Zweier C. 2017. FOXP2 variants in 14 individuals with developmental speech and language disorders broaden the mutational and clinical spectrum. *J Med Genet* **54**:64–72.

Rueden CT, Schindelin J, Hiner MC, DeZonia BE, Walter AE, Arena ET, Eliceiri KW. 2017. ImageJ2: ImageJ for the next generation of scientific image data. *BMC Bioinformatics* **18**:529.

Santos ME, Athanasiadis A, Leitão AB, DuPasquier L, Sucena E. 2011. Alternative splicing and gene duplication in the evolution of the FoxP gene subfamily. *Mol Biol Evol* **28**:237–247.

Schatton A. 2018. FoxP in Bees and Flies-conservation at Different Levels?: An Analysis of Sequence, Neurons, Circuits and Behavior (PhD). Freie Universität Berlin.

Schatton A, Agoro J, Mardink J, Leboulle G, Scharff C. 2018. Identification of the neurotransmitter profile of AmFoxP expressing neurons in the honeybee brain using double-label in situ hybridization. *BMC Neurosci* **19**:69.

Schatton A, Scharff C. 2017. FoxP expression identifies a Kenyon cell subtype in the honeybee mushroom bodies linking them to fruit fly αβc neurons. *Eur J Neurosci* **46**:2534–2541.

Schatton A, Scharff C. 2016. Next stop: Language. The "FOXP2" gene's journey through time. *Mètode* **0**. doi:10.7203/metode.7.7248

Seelig JD, Jayaraman V. 2015. Neural dynamics for landmark orientation and angular path integration. *Nature* **521**:186–191.

Serway CN, Kaufman RR, Strauss R, de Belle JS. 2009. Mushroom bodies enhance initial motor activity in Drosophila. *J Neurogenet* **23**:173–184.

Shan Q, Wang Y, Li J, Zhang Y, Chen K, Liang Z, Zhang K, Liu J, Xi JJ, Qiu J-L, Gao C. 2013. Targeted genome modification of crop plants using a CRISPR-Cas system. *Nat Biotechnol* **31**:686–688.

Shi Z, Luo G, Fu L, Fang Z, Wang X, Li X. 2013. miR-9 and miR-140-5p target FoxP2 and are regulated as a

function of the social context of singing behavior in zebra finches. *J Neurosci* **33**:16510–16521.

Shu W, Lu MM, Zhang Y, Tucker PW, Zhou D, Morrisey EE. 2007. Foxp2 and Foxp1 cooperatively regulate lung and esophagus development. *Development* **134**:1991–2000.

Strauss R, Hanesch U, Kinkelin M, Wolf R, Heisenberg M. 1992. No-bridge of Drosophila melanogaster: portrait of a structural brain mutant of the central complex. *J Neurogenet* **8**:125–155.

Sun J, Xu AQ, Giraud J, Poppinga H, Riemensperger T, Fiala A, Birman S. 2018. Neural Control of Startle-Induced Locomotion by the Mushroom Bodies and Associated Neurons in. *Front Syst Neurosci* **12**:6.

Su T-S, Lee W-J, Huang Y-C, Wang C-T, Lo C-C. 2017. Coupled symmetric and asymmetric circuits underlying spatial orientation in fruit flies. *Nat Commun* **8**:139.

Szüts D, Bienz M. 2000. LexA chimeras reveal the function of Drosophila Fos as a context-dependent transcriptional activator. *Proc Natl Acad Sci U S A* **97**:5351–5356.

Teramitsu I, White SA. 2006. FoxP2 regulation during undirected singing in adult songbirds. *J Neurosci* **26**:7390–7394.

Thompson CK, Schwabe F, Schoof A, Mendoza E, Gampe J, Rochefort C, Scharff C. 2013. Young and intense: FoxP2 immunoreactivity in Area X varies with age, song stereotypy, and singing in male zebra finches. *Front Neural Circuits* **7**:24.

Thum AS, Gerber B. 2019. Connectomics and function of a memory network: the mushroom body of larval Drosophila. *Curr Opin Neurobiol* **54**:146–154.

Turrel O, Goguel V, Preat T. 2018. Amnesiac Is Required in the Adult Mushroom Body for Memory Formation. *J Neurosci* **38**:9202–9214.

Usui N, Co M, Harper M, Rieger MA, Dougherty JD, Konopka G. 2017. Sumoylation of FOXP2 Regulates Motor Function and Vocal Communication Through Purkinje Cell Development. *Biol Psychiatry* **81**:220–230.

Warth Pérez Arias CC, Frosch P, Fiala A, Riemensperger TD. 2020. Stochastic and Arbitrarily Generated Input Patterns to the Mushroom Bodies Can Serve as Conditioned Stimuli in. *Front Physiol* **11**:53.

Weigel D, Jürgens G, Küttner F, Seifert E, Jäckle H. 1989. The homeotic gene fork head encodes a nuclear protein and is expressed in the terminal regions of the Drosophila embryo. *Cell* **57**:645–658.

Widmer YF, Fritsch C, Jungo MM, Almeida S, Egger B, Sprecher SG. 2018. Multiple neurons encode CrebB dependent appetitive long-term memory in the mushroom body circuit. *Elife* **7**. doi:10.7554/eLife.39196

Xie K, Minkenberg B, Yang Y. 2015. Boosting CRISPR/Cas9 multiplex editing capability with the endogenous tRNA-processing system. *Proc Natl Acad Sci U S A* **112**:3570–3575.

Xiong Y, Lv H, Gong Z, Liu L. 2010. Fixation and locomotor activity are impaired by inducing tetanus toxin expression in adult Drosophila brain. *Fly* **4**:194–203.